

Response to the referees' comments

- 5 We thank the referees for useful comments. Their comments are in italics, followed by our responses in Arial font and our changes to the manuscript in Times-Roman font.

10 In addition to responding to the referees' comments, we have also expanded the discussion of global missing OH reactivity in the MBL, improved some of the wording and consistency, and corrected typos.

Anonymous Referee #1.

- 15 *This paper presents OH reactivity measurements from the ATom aircraft project, providing a substantial dataset in the under-studied marine boundary layer which will no doubt help to improve our understanding of the global oxidation capacity. A comparison of measured OH reactivity with modelled OH reactivity in this region seems to demonstrate that there is missing OH reactivity and the authors attribute this to an ocean source of short-lived reactive gases. As well as a number of minor comments, I have a few queries on the*
20 *analyses performed to demonstrate that the missing OH reactivity in the MBL is statistically significant. Once these questions have been addressed, I am suggesting this manuscript is published in ACP.*

Pg 1, line 36: Define OHR

- 25 It is now defined as "OH Reactivity" in the abstract and again in the first paragraph of section 2.2.

Pg 1, line 38: Calculated or modelled OH reactivity?

- 30 We removed the words "value of" to say "The mean measured OH reactivity ...".

The amount of 'missing' reactivity often depends on the completeness of the individual OH sinks that were measured alongside. Although not the primary focus of this paper, it would be informative to know if the OH reactivity budget could be closed in the boundary layer over land?

- 35 Thanks to the referee for this suggestion. We have added a Section 3.3 OH Reactivity Over Land and have included the measured and missing OH reactivity values per dip in a new version of Figure 7. The new text is the following:

- 40 "Of the approximately 120 dips in which OH reactivity measurements were made, 14% were over land (Figure 7). The majority of these were made in the Arctic, several over snow, ice, and tundra. As a result, the median calculated OH reactivity was only 1.35 s^{-1} , while the median measured OH reactivity was 1.4 s^{-1} and the median

45 missing OH reactivity was -0.1 s^{-1} , which is essentially zero to well within uncertainties. Note, however, that there is little missing OH reactivity over most of the Arctic polar oceans as well as over the Arctic land, which means that missing OH reactivity is generally low over the entire colder Arctic region. The greatest measured missing OH reactivity was found on only one dip over the Azores, where the missing OH reactivity was $\sim 2.5 \text{ s}^{-1}$ larger than the calculated OH reactivity.”

50 Unfortunately, these measurements do not provide contribute to the evidence supporting the hypothesis that the missing OH reactivity over the oceans is due to ocean gaseous emissions because they were primarily in the Arctic where there was little missing OH reactivity.

55 *Pg 3, paragraph 3: Given the sparsity of MBL OH reactivity observations, I suggest the authors expand their discussion (in section 4 on the earlier Mao et al study) to include the Pfannersill et al study which reports higher MBL OH reactivities and higher missing OH reactivities than observed during ATom.*

60 Pg 3, paragraph 2 was already devoted to discussing the Pfannersill et al. study. We have enhanced it by adding more detail:

65 “One regime that has yet to be adequately investigated is the remote marine boundary layer (MBL) and the free troposphere above it, which comprises 70% of the global lower troposphere. Two prior studies measured OH reactivity in the MBL. The most recent was shipborne across the Mediterranean Sea, through the Suez Canal, and into the Arabian Gulf in summer 2017 (Pfannerstill et al., 2019). Several portions of this journey were heavily influenced by petrochemical activity or ship traffic, while others were relatively clean. Median measured OH reactivity for the different waterways ranged from 6 s^{-1} to 13 s^{-1} , while median calculated OH reactivity ranged from 2 s^{-1} to 9 s^{-1} . When more than 100 measured chemical species were included in the calculated OH reactivity, the difference between the measured and calculated OH reactivity was reduced to being with measurement and calculation uncertainty for some regions, but significant missing OH reactivity remained for other regions. In the cleaner portions of the Mediterranean and Adriatic Seas, the calculated OH reactivity of $\sim 2 \text{ s}^{-1}$ was below the instrument’s limit of detection (LOD = 5.4 s^{-1}).”

75 We note that essentially all ATom OH reactivity measurements in the MBL were far below the LOD of the instrument used in the Pfannerstill et al. research.

Table 2: Was NO₂ measured during the project? If it was, but was not used to constrain the model, could the authors provide a comment on the level of agreement between measured and modelled NO₂?

80 NO₂ was measured and is now included in Table 2. Measured NO₂ did not always agree with modeled NO₂ by as much as 30-50%. However, with a few exceptions, NO₂ was less than 40 pptv and accounted for less than 0.5% of the total calculated OH reactivity. Therefore, any issue with NO₂ has a negligible effect on the calculated OH reactivity.

85 *Pg 5, line 140: ‘background signal’ I presume the authors mean the ‘OH offline’ signal?*

As it reads, however, this 'background signal' may be confused with kbackground.

We agree with the referee and have changed the sentence to read: "...while the OH detection system switches the laser wavelength to off resonance with OH to measure the signal background."

90

Pg 5, line 141: Did the ratio of the flow of carrier gas to the flow of ambient air vary with altitude? If it did, the authors should comment on the impact impurities in the carrier gas may have at high and low altitudes respectively. Could a change in the flow ratios explain the observed pressure dependence presented in Fig 2?

95

We thank the referee for this question. The ratio of the wand flow, which is constant, to the total reaction tube flow does change with pressure, resulting in an increase in the hypothesized contaminant concentration with increasing pressure (i.e., decreasing altitude). In fact, the differences in the two fitted curves in Figure 2 can be mainly explained by this pressure dependence. We have added a paragraph after paragraph 6 in Section 2.2 that says:

100

"The difference in the linear fit to the offset calibration for ATom1 and ATom 4 and the linear fit to the offset calibration for ATom2 and ATom3 is pressure dependent (Fig. 2). The standard volume airflow in the wand was constant, but the ambient volume flow in the flow tube decreased by a factor of ~2 as the flow tube pressure increased from 30 kPa to 100 kPa. As a result, the contamination concentration from the wand air also increased a factor of ~2 as flow tube pressure increased. This pressure-dependent contamination concentration explains much of the difference between the two fitted lines and provides evidence that contamination in the wand flow was a substantial contributor to the changes in the zero offset between ATom1/ATom4 and ATom2/ATom3. The good agreement between the fit for ATom2/ATom3 and the offset calibrations of Mao et al. (2009), who used ultra-high purity N₂, suggests that the zero air for ATom2 and ATom3 had negligible contamination."

105

110

Pg 5, line 148: what NO concentration do the authors class as 'high NO'?

We change this statement to "...in environments where NO is greater than a few ppbv, ..."

115

Pg 5, line 156: Do the authors expect the low molecular weight VOCs present in the PAM chamber to form particles?

No, we do not. But our experience is that when there are low-molecular weight VOCs in contaminated ambient air, there are also higher molecular-weight VOCs as well. We have also added a sentence describing another test that we neglected to mention, which was to do some runs with high-purity N₂ as a comparison. The results were the same, but the PAM chamber test proved to be the more sensitive of the two. We add a sentence:

120

"The results of this test were consistent with those obtained by substituting the air from the zero air generator with high purity nitrogen."

125

Pg 5, line 159: What do the authors mean by 'media'

130 We add a parenthetical statement: “(Perma Pure ZA-Catalyst – Palladium on Aluminum Oxide)”.

130 *Pg 6, line 198: Was a pressure dependent background applied to all the OH reactivity data?*

Yes.

135 *Pg 7, line 209: ‘..only 0.2 s-1’ vs Pg 6, line 187: ‘0.25 – 0.3 s-1’*

140 One is the calculated OH reactivity using the flow tube pressure and temperature and the other is the calculated OH reactivity using ambient pressure and temperature. We now make this difference clear by changing the one on line 209 to “The OH reactivity from the model at the ambient temperature and pressure rarely exceeded 2 s^{-1} in the planetary boundary and was only 0.2 s^{-1} in the free troposphere.”

145 *Pg 7, section 2.3: How are photolysis rates treated in the model?*

150 The measured photolysis rates were used in the model to calculate the unmeasured but modeled chemical species. To get the calculated OH reactivity at the flowtube temperature and pressure, the model was initialized by constraining the measured and modeled chemical species for each time step and then running the model at the flow tube temperature and pressure for 1 second at a fixed OH value in order to generate the rate coefficients and concentrations needed to calculate the OH reactivity that would have been seen in the flow tube conditions.

155 *Pg 9, line 279: ‘Some extreme outlier points were removed..’ the authors should comment on the approach they chose to remove data – was this data flagged as potentially having a problem?*

160 We no longer remove any points before doing the correlations. This difference in approach changes the correlation values somewhat but did not change the variables for which the correlations are most significant.

Pg 9, line 287 and figure 4: Some of the OH reactivity data measured above 10 km do not match the model calculated OH reactivity exactly. Why?

165 We made the mean value of the measured OH reactivity and the mean value of the calculated OH reactivity the same over the altitude range from 10-12 km, but that does not mean that they will be the same at every altitude between 10 km and 12 km.

170 *Pg 9, line 292: Do the authors expect ambient HO2 to make it into the flow tube without being lost on inlet lines? Given the fast rate coefficient employed in the model for the*

reaction of $\text{CH}_3\text{O}_2+\text{OH}$, did CH_3O_2 not contribute a significant sink for OH?

175 The contributions to the calculated OH reactivity by HO_2+OH and $\text{CH}_3\text{O}_2+\text{OH}$ are comparable
and small. In the lowest 2 km, they contribute less than 3% to the mean total calculated OH
180 reactivity. Assuming that HO_2 and CH_3O_2 are lost in the OHR instrument and its sampling
lines, we plotted the missing OH reactivity with their contributions subtracted. The differences
in the plots was barely perceptible and none of the numbers for statistical significance or
correlations changed. We do not know for certain that these radicals are lost in the instrument
or sampling lines, however we do know that sticky chemical species such as HCHO, HOOH,
and CH_3OOH have no measurable loss. Thus, we choose to retain the figures without this
correction. In Section 3 Results, we add the sentence:

185 "It is possible that HO_2 and CH_3O_2 are lost in the Teflon sampling lines or the OHR instrument before they can
be measured, but their mean contribution to the calculated OH reactivity is less than 3% and can be ignored in
our analysis."

Pg 10, line 309: 4 km is much higher than the MBL and for ATom 3 there seems
to be statistically significant missing OH reactivity up to 6 km (fig 5). Was there any
190 evidence of long-range transport of pollution in these regions that could contribute to
OH reactivity (and missing OH reactivity) during these flights?

195 Pollution plumes were encountered over a range of altitudes during the missions. It is possible
that these few points are due to missing OH reactivity in those encounters, but it is also
possible are just statistical outliers due to aircraft maneuvers, short-lived instrument issues,
or clouds. We will look at these when we do an analysis of individual flights.

200 Pg 10, line 321: The authors should also comment of the 8 – 12 km data in figure
6. Some of these points also lie above the red dashed line. The number of 8 – 12
km points lying above the line is less than in the 0 – 4 km data, but is this simply
because the 10 – 12 km data was set to match the modelled reactivity? I suggest that
this analysis is conducted on 8 – 10 km data only and also 0 – 2 km and 2 – 4 km
separately.

205 Matching the means of the measured and calculated OH reactivity for data above 10 km has
nothing to do with the deviations from the normal distribution in the Q-Q plot. Thus using 10-12
km is appropriate, although we have changed this range to being above 8 km. The Q-Q plots
for 8-10 km and 10-12 km are very similar. So we will use 8-12 km for the counterexample on
the distribution. We also focus on 0-1 km, which is closest to the height of the MBL but still
contains enough data.

210 Pg 11, fig 7: I don't think the trend in missing reactivity with latitude is best illustrated
by figure 7. Do the authors see a reasonable correlation if they plot missing reactivity

vs latitude in a scatter plot?

215 We have now added a plot of per-dip missing OH reactivity as a function of latitude (Figure 8) in addition to the global view in Figure 7. We think that both have value.

Pg 11, line 339: *The authors should make it clear which figure these data have been included in.*

220

Done

Pg 12, line 367: *What were the typical NO concentrations during the campaigns? Table 3: I presume that the reactions from line 3 onwards apply to both Case 1 and Case 2?*

225 *As the Table is set out, however, it currently looks like only 1 reaction ($X + OH = XO_2$) is added for Case 1. If ' $XO_2 + NO = HO_2$ ' is included as a reaction, shouldn't ' $HO_2 + NO = OH$ ' also be considered?*

230 $HO_2 + NO$ is in MCMv331, so it does not need to be added. NO in the lowest 2 km was 7 ± 7 pptv, very low. If $X + OH$ is not important, then nothing in the subsequent chemistry is going to be important because the production of X is not going to be important. You can think of $X + OH$ as representing that reaction and all the subsequent reaction as far as OH reactivity goes.

Pg 13, line 392: *I think the authors mean 'missing' reactivity here.*

235

Fixed.

Pg 13, 405 onwards: *To determine the source strength, both the lifetime and the ambient concentration of the two species needs to be considered. So, although the calculated concentration of the alkane is 43 times greater than the calculated concentration of the sesquiterpene, the lifetime of the alkane is 43 longer, so the source strength to maintain the calculated concentrations of both species should be the same.*

240

The referee is correct.

245

We modify the paragraph:

250 "If the unknown VOC is an alkane with a reaction rate coefficient with OH of $2.3 \times 10^{-12} \text{ cm}^3 \text{ s}^{-1}$, then an unlikely large oceanic source of 340 Tg C yr^{-1} would be necessary (Travis et al., 2020). Adding this much additional VOC reduces global modeled OH 20-50% along the flight tracks, degrading the reasonable agreement with measured OH. Large sources of long-lived unknown VOCs, which do not have as large an impact on modeled OH, are also necessary to reduce but not resolve the discrepancies between measured and modeled acetaldehyde, especially in the Northern Hemisphere summer. These issues between a global model and measured missing OH reactivity and acetaldehyde need to be resolved."

Pg 13, line 407: *the Travis et al., 2019 is missing from the reference list.*

255

Travis et al., 2020, was recently submitted to ACPD. It is now listed in the references.

Pg 13, line 412: 's-1' - superscript '-1'

260 Fixed

Pg 13, line 413: '0.5 ppb' or '0.26 ppb'?

Fixed

265

270 *Thames and co-authors present OH reactivity measurements over the remote oceans
from the ATom campaigns. They use a 0D box model constrained to other ATom observations
to interpret the OHR data, specifically focusing on 'missing' OHR in the marine boundary layer.
The dataset is the first of its kind, spanning the globe, and is collected under analytically
challenging conditions (very clean air). The team is to be commended for the work that went
into collecting this dataset. It represents a great contribution to the community that I expect will
275 be used by many future researchers.*

*My main comments on the manuscript have to do with its treatment of uncertainties and
statistics. Since we are looking at very low OHR conditions, the missing OHR values
are also low and pushing the uncertainty limits. I feel that the paper needs a more
sophisticated and robust treatment of uncertainty statistics (including in the modeled
280 OHR, which is itself constrained to measurements) in order to provide a convincing
case that the missing OHR values are indeed robust. Once that is done the paper
should be published in ACP.*

=====

General comments

285 =====

*Along with uncertainties in the OHR measurement itself, the "modeled" OHR also has
uncertainties. It is constrained to trace gas measurements, which have their own uncertainties.
It predicts unmeasured species using rate coefficients that have uncertainties. It seems to me
that in order to judge whether the missing OHR is statistically robust, these uncertainties need
290 to be fully propagated through the modeled OHR derivation. Then one could do a proper
statistical comparison of the measured and modeled OHR values.*

We agree and have done a much more thorough analysis of all the uncertainties. We answer
this question about the model uncertainty and the measurement uncertainty together as an
295 answer to the line 180-184 comments.

*164: "these variations were tracked with measurements of the OHR instrument background in
the laboratory". I am confused by this because an earlier statement (line
141) appears to indicate that the background was measured every measurement cycle.
300 Please clarify.*

The confusion results from our using the word 'background' for two different measurements.
We now state (old line 141): "the OH detection system switches the laser wavelength to off resonance with
OH to measure the signal background." to make it clear that its background is in the laser signal. We
305 have renamed the OH reactivity instrument background as the "offset" throughout the
manuscript for consistency.

The first sentence in Section 2.3 now reads:

310 “The OHR offset varied between the 4 ATom phases due to changes in the zero-air generator performance and between research flights due to internal contamination from pre-flight conditions. These changes were tracked with measurements of the OHR instrument offset in the laboratory and, for ATom4, in situ during several flights.”

315 *180-184: how can we be confident that the pressure dependence of the calibration is prescribed accurately enough to define (for example) a mean 0.5 1/s discrepancy? The relatively large amount of scatter in Figure 2 (e.g., for the ATom-1/4 calibration) by itself does not by itself inspire confidence in this respect. Given the small OHR discrepancies that are discussed later, I feel the paper needs a more rigorous discussion of the background and calibration uncertainties, along with a quantitative analysis of how these propagate onto the end results, for us to have confidence in the findings.*

320 *It doesn't appear that a pressure-dependent calibration curve was performed at the time of ATom-1. How are we confident that the 2018 curve fits the ATom-1 data given the 2-year separation in time?*

325 We have extensively re-analyzed our OHR offset data and better quantified our estimate the total uncertainty in the missing OH reactivity measurements. We created a new Section 2.3 OH reactivity measurement offset calibrations and another new Section 2.4 Missing OH reactivity uncertainty analysis.

330 We need to stress that doing the in-flight offset calibration was extremely difficult, involving crawling into the forward cargo bay of an aircraft bouncing 500 ft above the ocean surface, all the while trying to adjust a regulator to keep the air flow in the OHR flowtube constant for three minutes as the cylinder pressure slowly decreases. We add the following to Section 2.3:

335 “The difficulty of maintaining steady calibration conditions in flight during ATom4 caused the large in situ calibration error. The standard deviation of these offset calibrations is 0.75 s^{-1} , which is 2.5 to 3 times larger than the SD obtained for ambient measurements in clean air for the same altitude and number of measurements, indicating that the atmospheric measurement precision is much better than could be achieved in these difficult offset calibrations. Yet even with this lower precision, the median offset at high and low pressure agree with the linear fit of the laboratory calibrations to within 20% at low pressures and 3% at high pressure.”

340

We are confident that the ATom1 pressure dependence is the same as that for ATom4 because of the excellent agreement at 100 kPa and the knowledge that the low pressure offset measurements in the laboratory, in situ for ATom4, and Mao et al. (2009) are all at or slightly above 2 s^{-1} . This similarity between ATom1 and ATom4 suggests that the contamination that plagued ATom4 also plagued ATom1.

345

We add the following in Section 2.3:

350 “For ATom1, the offset was calibrated at only 97 kPa prior to the mission, but it is in excellent agreement with the offset calibrated for ATom4. We can safely assume that the ATom4 offset slope can be applied to ATom 1

because all offset calibrations performed at low OHR flowtube pressures, even those of Mao et al. (2009), are ~ 2 s⁻¹.”

355 *190-194: A pressure-invariant offset is being applied to the measurements based on
model output for the upper free troposphere. Please indicate the magnitude of this
offset that is being applied (e.g., compared to the inferred missing OHR magnitudes
that are discussed later). Is there reason to believe that this offset is in fact pressure
independent as assumed?*

360 This paragraph has been rewritten with the following explanation:
“The OHR offset varied slightly from flight to flight because the variable air quality produced by the zero-air
generator. This flight-to-flight variation was tracked and the OH reactivity offset was corrected by the following
procedure. The OH reactivity calculated from the model at the OHR instrument’s temperature and pressure (sec
365 Sect 2.3) was 0.25-0.30 s⁻¹ for the upper troposphere during all ATom phases and latitudes. The offset
calibrations were adjusted in the range of 0.34±0.32 s⁻¹ for each research flight by a pressure-invariant offset that
was necessary to equate the median measured and model-calculated OH reactivity values for data taken above 8
km altitude. If this offset correction is not used for all altitudes, then the OH reactivity in the 2- 8 km range varies
unreasonably from flight-to-flight, even going significantly negative at times. In effect, we used the upper
370 troposphere as a clean standard in order to fine-tune k_{offset} , just as Mao et al. (2009) did.”

*207-208: “Therefore, in each ATom phase, the total uncertainty in the OH reactivity is
dominated by the instrument background uncertainty.” My interpretation of this is that
375 we should be considering the errors as primarily systematic rather than random. I.e.,
the campaign-specific background at any given pressure is a single constant quantity
that we can define to 1-sigma of 0.4 1/s. And therefore that uncertainty is not reduced
by temporal averaging of the campaign measurements: the background uncertainty
is the same (0.4 1/s) whether we are considering 1 measurement or thousands. Is
380 my interpretation correct? If so then I don’t believe 1-sigma is an appropriate metric,
since sigma is a measure of variability rather than of certainty about the central value.
A more appropriate metric would be the 95% confidence interval about the pressure
dependent backgrounds – for example, obtained via bootstrap analysis of the data in
Figure 2.*

385 We have completely revised this analysis and description. We agree that systematic (i.e.,
absolute) errors affect the missing OH reactivity values and use our knowledge of
uncertainties in the several components going into the missing OH reactivity calculation to
perform a sensitivity (i.e. error propagation) analysis. This description has become the first
390 paragraph in the new Section 2.4:

“The uncertainty for missing OH reactivity in the MBL at the 68% confidence level comes from four components: the decay
measurement itself; the offset as determined by the slope and intercepts of the fits to the laboratory OH reactivity offset
calibrations (Fig. 2); the flight-to-flight offset variation as judged by fitting the measured OH reactivity to the model-

395 calculated OH reactivity at 8-12 km altitude; and the model calculations. First, the uncertainty in decay fit is approximately $\pm 7.5\%$, which for a typical OH reactivity measurement in the MBL of $\sim 2 \text{ s}^{-1}$, would give an uncertainty of $\pm 0.15 \text{ s}^{-1}$.
Second, the uncertainty in the OH reactivity offset in the MBL is found from the sum of the slope uncertainty times the OHR flow tube pressure, which is $\sim 100 \text{ kPa}$ in the MBL, ($\pm 0.16 \text{ s}^{-1}$) and the intercept uncertainty ($\pm 0.11 \text{ s}^{-1}$). The two
400 uncertainties are assumed to be correlated. Third, the uncertainty in the flight-to-flight offset variation is the standard deviation of the mean for each high altitude short level leg ($\pm 0.15 \text{ s}^{-1}$). Fourth, the uncertainty of the model-calculated OH reactivity was determined by Eq. 4:

$$\Delta k_{OH}^{calc} (\text{s}^{-1}) = \sqrt{\sum [(k_i \Delta x_i)^2 + (\Delta k_i x_i)^2]} \quad (4)$$

405 where k_i are the reaction rate coefficients and x_i are the OH reactant concentrations. The rate coefficient uncertainties come from Burkholder et al. (2016) and the chemical species uncertainties come from Table 2 and Brune et al. (2020). For the 11 chemical species responsible for 95% of the total OH reactivity in the MBL, this uncertainty is $\pm 0.08 \text{ s}^{-1}$. The square root of the sum of the squares of all these uncertainties yields a total uncertainty for the MBL missing OH reactivity of $\pm 0.32 \text{ s}^{-1}$ at the 68% confidence level.”

410 Note that this more careful calculation of the mOHR absolute uncertainty is somewhat less than our earlier estimate of $\pm 0.4 \text{ s}^{-1}$.

415 299: “The median measured OH reactivity equals the median model-calculated OH reactivity to within 1 statistical uncertainty”, see above, sigma is a measure of scatter rather than uncertainty

420 The confidence level is directly related to the probability of occurrence, which is measured by the standard deviation in a normal distribution, if the uncertainty is approximately normally distributed. None-the-less we have changed our notation on the confidence levels to percentages.

425 Figure 2, “Darker grey points indicate OH reactivity values greater than the 1-sigma uncertainty in the MBL.” Wording is unclear here. At first I thought it meant “missing OH reactivity values greater than the 1-sigma: : .”, but from the plot it looks like the colored values are just those where the actual OH reactivity is 1-sigma above the median value. Please clarify.

Removed.

430 305-311 and Figure 5: There is some conflation of spread and uncertainty here. First, the “For missing OH reactivity to be meaningful, some missing OH reactivity points must be much greater than the statistical spread of the OH reactivity measurements.” A bit oddly worded, rather one should say that to be meaningful, the missing OH reactivity
435 should exceed the statistical uncertainty of the OH reactivity measurements. Spread and uncertainty are not the same thing. Similarly, in the Figure 5 caption: “Dotted black lines represent +/-2-sigma uncertainty derived from a median of the missing OH reactivity values greater than 4 km.” If the lines are just twice the SD they are showing the spread, not

440 *the uncertainty. And wording-wise it is not clear what “2-sigma uncertainty derived from a
median” means. Finally, “About 95% of all points above 4 km are within that phase’s 2
uncertainty bands, which is consistent with a statistically normal distribution.” – again mixing
up variability with uncertainty.*

445 We have redone the analysis and made it much more rigorous and statistically sound. This
section has been extensively rewritten:

“3.2 Missing OH Reactivity: Statistical Evidence

450 A better approach is to find the missing OH reactivity for each measurement time point and then look at the mean
values. The missing OH reactivity is plotted as a function of altitude for ATom1, ATom2, and ATom3 (Fig. 5).
The mean missing OH reactivity is set to 0 s^{-1} for 8-12 km, but remains near to 0 down to 2-4 km, where it then
increases. The 1-minute measurements are a good indicator of the measurement precision, which is $\pm 0.35 \text{ s}^{-1}$ for
ATom1 and $\pm 0.25 \text{ s}^{-1}$ for ATom2 and ATom3.

455 In the MBL, the mean missing OH reactivity is 0.4 s^{-1} for ATom1, 0.5 s^{-1} for ATom3, 0.7 s^{-1} for ATom2. From a
Student t-test in which the MBL missing OH reactivity is compared to either the values at 6-8 km or 8-12 km
altitude ranges, the differences in mean missing OH reactivity between the MBL and the higher altitudes is
statistically significant for a significance level, α , equal to 0.01, with p-values $< 10^{-15}$. However, the mean MBL
missing OH reactivity values are close to the upper limit on the absolute missing OH reactivity uncertainty (95%
confidence), which is 0.64 s^{-1} (blue bar, Fig. 5). There is a small probability (2-10%) that the mean MBL missing
OH reactivity is due only to absolute error in the missing OH reactivity measurement that was derived in Section
460 2.4.

465 The mean MBL missing OH reactivity contains measurements for which the missing OH reactivity is 0 s^{-1} . The
real interest is in the missing OH reactivity that greater than can be explained by absolute missing OH reactivity
measurement error or precision. From Fig5., it is clear that the positive scatter of data is much greater than the
negative. The means of standard deviations of the negative values and of the positive values were calculated for
1-km height intervals (dashed lines). These lines and the individual data points both indicate skewness in the
missing OH reactivity, especially in the lowest 2-4 km altitude. A skewness test shows that, in and just above the
MBL, missing OH reactivity from ATom1 and ATom2 exhibit weak-to-moderate skewness (~ -0.4) in the MBL
while from ATom2 exhibits strong skewness (1.4).”

470 *313-327 and Figure 6: This (qq-plots and t-test) is a nice demonstration that the missing
OHR data above and below 4km follow differing statistical distributions. Please
discuss the robustness of this finding in view of i) the statistical uncertainty of the
pressure-dependent background corrections in Figure 2, ii) the propagated uncertainty
475 in the modeled OHR, and iii) the assumption of a pressure-invariant offset (line 190-
194). Second, the figure is only showing ATom-2 data but the text (by not mentioning
this) implies that all of the data from ATom-1, 2, and 3 have this feature. Is that the
case?*

480 The previous section continues with a discussion of the Q-Q plots:

“Quantile-quantile plots (Q-Q plots) provide a visual description of the relationship between a sample distribution and a normal distribution. If the sample is perfectly normally distributed, then its values will lie along a straight line. Data lying higher than the line for values on the right side of the normal distribution (positive standard normal quantiles) indicate more high-value data than expected, while data higher than the line for values on the left side of the normal distribution indicate fewer low-value data than expected.”

Quantile-quantile plots (Q-Q plots) provide a visual description of the relationship between a sample distribution and a normal distribution. The standard normal quantiles are plotted on the x-axis and the sample quantiles on the y-axis. If the sample is perfectly normally distributed, then its values will lie along a straight line. Data lying higher than the line for values on the right side of the normal distribution (positive standard normal quantiles) indicate more high-value data than expected, while data higher than the line for values on the left side of the normal distribution (negative standard normal quantiles) indicate fewer low-value data than expected.

Q-Q plots are shown for three ATom2 cases in Fig. 6. The large boxes are the interquartile range between the 1st quartile (25% of the data below it) to the 3rd quartile (75% below). The missing OH reactivity data for altitudes greater than 8 km (red data) is normally distributed until the standard normal quantile of 2, meaning that less than a few percent of the data is higher than expected. On the other hand, the missing OH reactivity data in the MBL (blue data) are normally distributed between standard normal quantiles of -2 and 1, meaning that a few percent of low-value are less than expected, but, more importantly, as much as 20% of the high-value data is greater than expected. Also included in Fig. 6 is the case for which we assume that the MBL missing OH reactivity zero value is actually greater by the missing OH reactivity absolute uncertainty at 95% confidence (gray data). Comparing these two MBL cases shows that changes in the mean missing OH reactivity values affect only the median value and not the distribution skewness. Q-Q plots for ATom1 and ATom2 (not shown) are less dramatic, but still have the same characteristics: for measurements above 8 km, the high-value data are more normally distributed; for the MBL, ~20% of high-value data are greater than expected.”

333-334: *“The latitudinal dependence implies that air or sea temperature or other latitude-dependent factors contribute to missing OH reactivity.” Also, the highest missing OHR values fall in the NH, implying that the generally higher abundance of trace gases in the NH plays a role : : : right?*

Removed.

342: “the main correlations that stand out are : : :” please be more precise in your language here, are these the 4 variables with the highest correlations?

This sentence has been rewritten:

“From the procedure given in Section 2.6, missing OH reactivity has the four strongest correlations with ...”.

342-350 and Figure 8: please discuss whether these correlations persist when the campaigns are considered individually.

525 Please see the discussion in Section 2.6. For the different ATom phases, the correlations
could be different with the much sparser individual data sets. The criteria used required
530 correlations for each ATom phase using both the pre-dip and pre-flight data sets. By requiring
correlations simultaneously for multiple methods, we are confident that we have found robust
correlations.

530 To see what the relationship is for different ATom phases, please look at the revised Figure 8.
In general, you can see the correlation for each phase by focusing only on its points.

535 *363: "the 1-sigma confidence level", please see earlier comments about confidence
intervals. What is needed here is a statement of whether the slopes agree to within
(say) 95% confidence based on a bootstrap / monte carlo test. In the same way, please
also indicate whether the slope is significantly different than zero.*

540 To find the absolute uncertainty, we chose to differentiate Eq. 3 and use propagation of error
analysis to get our absolute uncertainty estimates, which is just as good as using the standard
deviation of a distribution obtained by Monte Carlo simulations.

545 We do not have the data for Mao et al. (2009) and so cannot find the uncertainty in the slope
and intercept to their fit. However, we add the uncertainties at the 95% confidence level (2σ on
a normal probability distribution) for the absolute missing OH reactivity uncertainty to show
that it is possible that the two observations are the same.

550 We did calculate the standard deviation of the slope for the ATom fit and have included it in
the figure. We have also revised the paragraph:
"The linear fit of the missing OH reactivity against HCHO data from Mao et al. (2009) is given as the solid red line in Fig. 9.
If instead the pressure-dependent offset is used for Mao et al. (2009), then the resulting missing OH reactivity against HCHO
follows the dashed red line. With the absolute INTEX-B offset uncertainty at $\pm 0.5 \text{ s}^{-1}$ and the absolute ATom offset
uncertainty at $\pm 0.32 \text{ s}^{-1}$, both at the 68% confidence level, the linear fits for missing OH reactivity against HCHO in ATom
and INTEX-B agree to within combined uncertainties. The ATom linear fit slope is only 2.7 standard deviations from the
555 INTEX-B slope, but is 4.4 standard deviations from a line with zero slope, making it highly unlikely that missing OH
reactivity is not correlated with HCHO. The INTEX-B and ATom slopes to the linear fits are not exactly the same. However,
given the uncertainties, the HCHO dependence of the adjusted missing OH reactivity found in INTEX-B is consistent with
that found for the ATom missing OH reactivity over the northern Pacific Ocean."

560 372-373: "become substantially less than observed" and "become greater than observed",
please be quantitative

We have revised the sentence:
"For case 1 in which there is no OH produced in the X oxidation sequence, the modeled OH and HO₂ become 30-
565 40% less than observed at altitudes below 2 km. On the other hand, if XO₂ and its products autoxidize to produce
OH (Crouse et al., 2013), then the modeled OH and HO₂ become 10-20% greater than observed."

My understanding is that the NO₂ measurements during ATom have high uncertainty.
Is that right? Are you using the measured NO₂ or is this being predicted by the model
570 from other species?

NO₂ was measured and is now included in Table 2. Measured NO₂ did not always agree with
modeled NO₂ by as much as 30-50%. However, with a few exceptions, NO₂ was less than 40
575 pptv and accounted for less than 0.5% of the total calculated OH reactivity. Therefore, any
issue with NO₂ has a negligible effect on the calculated OH reactivity.

=====
Minor / technical / language corrections
=====

580 *There are some minor grammatical errors throughout; please do a careful proofreading.*

29: *"which IS 0.5 s-1 larger"*
Fixed.

35-36: *"for much of the free troposphere", awkward, suggest "throughout much : : :"*
585 We think this statement is fine as it is and are leaving it unchanged,

45: *suggest "with THE hydroxyl RADICAL"*
Changed.

590 46-47: *"is lost by the sum of the reaction frequencies", wording is not quite right b/c the
loss is via the chemical reactions themselves, the frequencies just determine how fast
that occurs. Suggest "is lost at a rate determined by the sum: : :"*
Corrected.

595 47: *suggest "This sum of loss frequencies is called: : :"*
Corrected.

68: *"exceeded the calculated AMOUNT by"*
"measured OH reactivity" is an amount. We will leave this sentence as is.

600 69: *VOC not defined*
Fixed

71: *"in A northern Michigan forest"*
605 Fixed

75: *"20%, which is approximately the uncertainty". But doesn't this percentage depend
on the absolute OHR amount?*

610 Yes, but the goal is to close the budget, no matter what the absolute amount is. So the
percentage is the most important quantity, not the absolute value for accomplishing this goal.

103: *as stated later this 0.4 1/s LOD is for 1-minute averages, consider specifying that here*

The new sentence is more specific:

615 “Although the calculated OH reactivity in the middle-to-upper troposphere is less than the OH reactivity instrument’s LOD, which is $\sim\pm 0.4 \text{ s}^{-1}$ for 1-minute averages when both absolute uncertainty and measurement variability are taken into account, this instrument can measure OH reactivity in and just above the MBL.”

620 149: *“in high NO environments”, please specify the approximate NO level at which this effect becomes relevant*

Done. It’s approaching 10 ppbv.

190: *“1-minute sums”, perhaps this should be “1-minute averages”*

625 Removed.

Figure 1: *I don’t know that it is helpful to include ATom-4 in this Figure given that the data is not ultimately used in the analyses that follow.*

We want to include it even if we do not use it in the analysis.

630

230: *“and other measurements were used to fill gaps in the primary measurement”.*

Can you please add a few words to be more specific here? E.g., “linear regression to other measurements”?

635 We basically just substituted one measurement for the other. It must be noted that with a few exceptions, the measurements that we had to substitute were in excellent agreement. We chose the ones with the highest resolution, but substituted in ones with slightly lower when the higher resolution measurements were not available. This substitution accounted for less than 10% of the total time.

640 250: *Need to specify assumed OH level giving this 1-hour lifetime*

We have modified this sentence to read:

“...which gives X a lifetime of about an hour for the typical daytime [OH] of $\sim 3 \times 10^6 \text{ cm}^{-3}$.”

645 Figure 2: *If I understand Figure 2 correctly, the blue fit is being used for both ATom-1 and ATom-4, is that correct? If so, the legend should be relabeled to make this more clear.*

The new figure caption now reads:

650 “Figure 2. Laboratory and in situ calibrations of OHR offset over 1-minute sums. The offset was calibrated only at $\sim 100 \text{ kPa}$ around ATom1 in 2015 and 2016 (black triangle). The offset was measured with a slightly different instrument configuration during the OH reactivity intercomparison study in 2015 (Fuchs et al., 2017). Offset

calibrations performed in 2017 between ATom2 and ATom3 (yellow starts with linear fit (yellow line), in 2018 at the end of ATom4 (red circles) and linear fit (red line), and in flight (blue dots with error bars indicating the range of 75% of the data) are shown. The ATom4 fit was used for ATom1 because the high-pressure laboratory calibrations were essentially the same.”

655 *Fig 2: “The median OH reactivity of 500m altitude bins is shown for measured OH reactivity (blue line, with 1 error bars)”, in fact the error bars are only shown at 2km increments, suggest clarifying in caption*
I believe that Referee #2 is referring to Figure 4. This figure and its caption have been redone.

660 *270: “These legs: : :” awkward wording*
We add the word “level” to be consistent with the wording in the preceding sentence.

270-271: suggest stating range of MBL heights during ATom.
665 We have corrected these sentences to read:
“Each per-dip bin is a single value representing an average of the missing OH reactivity as the DC-8 flew a level leg at 160 m. These level legs were generally well in the MBL because its height was greater than 160 m 85% of the time.”

670 *290: some representative OHR ranges would be helpful here.*
We have added the non-restrictive qualifier: “which is typically 10-50 s⁻¹.” after the reference.

318: “The missing OH reactivity values measured below 4 km altitude lie along the red dashed line” I think you mean “above 4 km” here.
675 This comment is no longer relevant because the plot and its description have been completely changed.

Figures 1, 4, 5, 7: I recognize that this information is also in Table 1, but it would be helpful to your reader if you indicated the time-frame of each ATom deployment somewhere on these figures.
680 We added the month in parentheses to the captions for Figs. 4, 5, and 7.

Table 1: a single season is given for each ATom deployment, but ATom covered both hemispheres.
685 We added “NH” to “Season” to make it clear.

336-340: do you suspect instrumental factors here?
No. We checked the raw decays very carefully and they were good.

690 *340: “While present on some figures”, please be specific*
The sentence now reads:
“While present on all figures except Fig. 8, they were not included in the correlation analysis.”

695 Figure 8, “at the per-flight time resolution” is unclear, I think you mean that each point
is an average over all the data for a given flight?

The caption now reads”

“Figure 8. The best correlations with missing OH reactivity for data at the per-flight resolution across all latitudes
and hemispheres. The symbols are per-flight data for ATom1 (circles), ATom2 (squares), ATom3 (diamonds).

700 Black lines are least squares fits to the per-flight data.”

356-357: wording is awkward here

The sentence has been reworded to read:

705 “The INTEX-B correlation coefficient between missing OH reactivity and HCHO ($R^2 = 0.58$) is better than the
one found for ATom ($R^2 = 0.35$), but in the range of ATom HCHO (100 pptv – 500 pptv), the ATom correlation
coefficient is larger.”

710

The number of changes is too extensive for a simple list. Please see the track-changes document for all
the changes.

715

Missing OH Reactivity in the Global Marine Boundary Layer

Alexander B. Thames¹, William H. Brune¹, David O. Miller¹, Hannah M. Allen², Eric C. Apel³, Donald R. Blake⁴, T. Paul Bui⁵, Roisin Commane⁶, John D. Crouse⁷, Bruce C. Daube⁸, Glenn S. Diskin⁹, Joshua P. DiGangi⁹, James W. Elkins¹⁰, Samuel R. Hall³, Thomas F. Hanisco¹¹, Reem A. Hannun^{11,12}, Eric Hints^{10,13}, Rebecca S. Hornbrook³, Michelle J. Kim⁷, Kathryn McKain^{10,13}, Fred L. Moore^{10,13}, Julie M. Nicely^{11,14}, Jeffrey Peischl^{10,15}, Thomas B. Ryerson¹⁵, Jason M. St. Clair^{11,12}, Colm Sweeney¹⁰, Alex Teng², Chelsea R. Thompson^{13,15}, Kirk Ullmann³, Paul O. Wennberg^{7,16}, and Glenn M. Wolfe^{11,12}

¹Department of Meteorology and Atmospheric Science, The Pennsylvania State University, University Park, PA, USA.

²Division of Chemistry and Chemical Engineering, California Institute of Technology, Pasadena, CA, USA.

³Atmospheric Chemistry Observations & Modeling Laboratory, National Center for Atmospheric Research, Boulder, CO, USA.

⁴Department of Chemistry, University of California, Irvine, CA, USA.

⁵Earth Science Division, NASA Ames Research Center, Moffett Field, CA, USA.

⁶Department of Earth and Environmental Sciences, Lamont-Doherty Earth Observatory, Columbia University, Palisades, NY, USA.

⁷Division of Geological and Planetary Sciences, California Institute of Technology, Pasadena, CA, USA.

⁸Department of Earth and Planetary Sciences, Harvard University, Cambridge, MA, USA.

⁹Chemistry and Dynamics Branch, NASA Langley Research Center, Hampton, VA, USA.

¹⁰Global Monitoring Division, NOAA Earth System Research Laboratory, Boulder, CO, USA.

¹¹Atmospheric Chemistry and Dynamics Laboratory, NASA Goddard Space Flight Center, Greenbelt, MD, USA.

¹²Joint Center for Earth Systems Technology, University of Maryland, Baltimore County, Catonsville, MD, USA.

¹³Cooperative Institute for Research in Environmental Sciences, University of Colorado, Boulder, CO, USA.

¹⁴Earth System Science Interdisciplinary Center, University of Maryland, College Park, MD, USA.

¹⁵Chemical Sciences Division, NOAA Earth System Research Laboratory, Boulder, CO, USA.

¹⁶Division of Engineering and Applied Science, California Institute of Technology, Pasadena, CA, USA.

Correspondence to: William H. Brune (whb2@psu.edu)

Abstract. The hydroxyl radical (OH) reacts with thousands of chemical species in the atmosphere, initiating their removal and the chemical reaction sequences that produce ozone, secondary aerosols, and gas-phase acids. OH reactivity, which is the inverse of OH lifetime, influences the OH abundance and the ability of OH to cleanse the atmosphere. The NASA Atmospheric Tomography (ATom) campaign used instruments on the NASA DC-8 aircraft to measure OH reactivity and more than 100 trace chemical species. ATom presented a unique opportunity to test the completeness of the OH reactivity calculated from the chemical species measurements by comparing it to the measured OH reactivity over two oceans across four seasons. Although, throughout much of the free troposphere, the calculated OH reactivity was below the limit-of-detection for the ATom instrument used to measure OH reactivity, the instrument was able to measure the OH reactivity in and just above the marine boundary

Deleted: Alexander B. Thames¹, William H. Brune¹, David O. Miller¹, Hannah M. Allen², Eric C. Apel³, Donald R. Blake⁴, T. Paul Bui⁵, Roisin Commane⁶, John D. Crouse⁷, Bruce C. Daube⁸, Glenn S. Diskin⁹, Joshua P. DiGangi⁹, James W. Elkins¹⁰, Samuel R. Hall³, Thomas F. Hanisco¹¹, Reem A. Hannun^{6,7}, Eric Hints^{10,12}, Rebecca S. Hornbrook³, Michelle J. Kim⁷, Kathryn McKain^{10,12}, Fred L. Moore^{10,12}, Julie M. Nicely^{6,7}, Jeffrey Peischl^{10,11}, Thomas B. Ryerson¹¹, Jason M. St. Clair^{6,7}, Colm Sweeney⁹, Alex Teng⁴, Chelsea R. Thompson^{10,11,12}, Kirk Ullmann³, Paul O. Wennberg³, and Glenn M. Wolfe^{6,7}. (... [1])

Deleted: four

Deleted: OH reactivity instrument's

Deleted: much of the free troposphere

Deleted:

Deleted: the OHR instrument

layer. The mean, measured value of OH reactivity in the marine boundary layer across all latitudes and all ATom deployments was 1.9 s^{-1} , which is 0.5 s^{-1} larger than the mean calculated OH reactivity. The missing OH reactivity, the difference between the measured and calculated OH reactivity, varied between 0 s^{-1} to 3.5 s^{-1} , with the highest values over the Northern Hemisphere Pacific Ocean. Correlations of missing OH reactivity with formaldehyde, dimethyl sulfide, butanal, and sea surface temperature suggest the presence of unmeasured or unknown volatile organic compounds or oxygenated volatile organic compounds associated with ocean emissions.

Deleted: average
Deleted: phases
Deleted: average
Formatted: Font:12 pt
Deleted: Concurrently, missing OH reactivity, the difference between the measured and calculated OH reactivity, was measured to be -0.5 - 2.0 s^{-1} at some locations in the tropics and midlatitudes

780 1 Introduction

The primary fate of the thousands of trace gases emitted into the atmosphere is chemical reaction with the hydroxyl radical (OH). While OH is produced primarily by the photolysis of ozone, followed by a reaction between excited-state atomic oxygen and water vapor, OH is lost at the rate determined by the sum of the reaction frequencies with these trace gases. This sum of loss frequencies is called the OH reactivity and has units of s^{-1} . If OH production remains constant, increases in OH reactivity will decrease the total atmospheric OH concentration. Thus, understanding global OH reactivity is a key to understanding global OH and the global atmospheric oxidation capacity.

Deleted: by
Deleted: es

An important example is methane (CH_4), which is removed from the atmosphere primarily by reaction with OH. Two estimates of the CH_4 lifetime due to oxidation by OH are 9.7 ± 1.5 years (Naik et al., 2013) and 11.2 ± 1.3 years (Prather et al., 2012). A recent global inverse analysis of GOSAT satellite CH_4 column emissions finds a CH_4 lifetime of 10.8 ± 0.4 years for oxidation by tropospheric OH (Maasakkers et al., 2019), which is within the uncertainties of the other two estimates. Understanding the CH_4 lifetime depends on understanding global spatial and temporal OH distributions, which are, strongly influenced by the spatial and temporal distribution of OH reactivity.

Deleted: is

OH reactivity is the inverse of the OH lifetime. It is calculated as a sum of OH reactant concentrations multiplied by their reaction rate coefficients:

Deleted: the reaction frequencies of
Deleted: s

$$k_{OH} = \sum_i k_{(OH+X_i)} [X_i]. \quad (1)$$

where $k_{(OH+X_i)}$ represents some species X's reaction rate coefficient with OH and $[X_i]$ is the concentration of that species. If there is no OH production, then the equation for the OH decay is

$$\frac{d[OH]}{dt} = -k_{OH}[OH]. \quad (2)$$

The first direct measurements of OH reactivity were made in Nashville, TN in summer 1999 (Kovacs et al., 2003). The measured OH reactivity exceeded the calculated by about 30%, which was thought to come from short-lived highly reactive volatile organic compounds (VOCs) that were not measured in that study. The difference between the measured and calculated OH reactivity was referred to as the "missing" OH reactivity. For forest environments, the first evidence for missing OH reactivity came from direct OH reactivity measurements in a northern Michigan forest in summer 2000 (Di Carlo et al.,

2004). As much as a third of the OH reactivity was missing, with missing OH reactivity increasing with temperature in a manner identical to the expected increase of forest monoterpene emissions. Since then, OH reactivity has been measured many times in various urban, rural, and forest environments (Yang et al., 2016, and references therein). The fraction of missing OH reactivity in different forests varies from less than 20%, which is approximately the uncertainty in the measured and calculated OH reactivity (Kaiser et al., 2016; Zannoni et al., 2016), to more than 50% (Nölscher et al., 2012; Nölscher et al., 2016). Considering the large numbers of trace gases emitted into the atmosphere (Goldstein and Galbally, 2007), it is possible that missing OH reactivity comes from OH reactants that were not measured or not included in previously calculated totals of the OH reactivity sum. In some studies, the OH reactants have been only those that were measured, and in other studies unmeasured but modeled OH reactants – such as organic peroxy radicals and oxygenated volatile organic compound (OVOC) products – have been included. A recent intercomparison of several OH reactivity instruments demonstrated that these large missing OH reactivity values are probably not due to instrument issues (Fuchs et al., 2017). These discrepancies have yet to be resolved.

One regime that has yet to be adequately investigated is the remote marine boundary layer (MBL) and the free troposphere above it, which comprises 70% of the global lower troposphere. Two prior studies measured OH reactivity in the MBL. The most recent was shipborne across the Mediterranean Sea, through the Suez Canal, and into the Arabian Gulf in summer 2017 (Pfanterstill et al., 2019). Several portions of this journey were heavily influenced by petrochemical activity or ship traffic, while others were relatively clean. Median measured OH reactivity for the different waterways ranged from 6 s^{-1} to 13 s^{-1} , while median calculated OH reactivity ranged from 2 s^{-1} to 9 s^{-1} . When more than 100 measured chemical species were included in the calculated OH reactivity, the difference between the measured and calculated OH reactivity was reduced to being with measurement and calculation uncertainty for some regions, but significant missing OH reactivity remained for other regions. In the cleaner portions of the Mediterranean and Adriatic Seas, the calculated OH reactivity of $\sim 2 \text{ s}^{-1}$ was below the instrument's limit of detection (LOD = 5.4 s^{-1}).

The other study involved airborne OH reactivity measurements made during the Intercontinental Chemical Transport Experiment Phase B (INTEX-B) study, a NASA airborne campaign investigating Asian-influenced pollution over the north Pacific Ocean in April-May, 2006 (Mao et al., 2009). In this study, aged pollution plumes from Southeast Asia were encountered within large regions of relatively clean air. At altitudes below $\sim 2 \text{ km}$, missing OH reactivity was $\sim 2.4 \text{ s}^{-1}$, more than the calculated OH reactivity of $1.6 \pm 0.4 \text{ s}^{-1}$. It decreased to within measurement uncertainty above 4 km . The correlation of missing OH reactivity with formaldehyde (HCHO) suggested that the missing OH reactivity was due to highly reactive VOCs that had HCHO as a reaction product. The confinement of the missing OH reactivity to the MBL and just above it suggested that the cause of the missing OH reactivity was ocean emissions of volatile organic compounds (VOCs).

In this paper, we describe measurements of OH reactivity that were made during the NASA Atmospheric Tomography (ATom) campaign (ATom, 2016). This campaign took place in four month-long phases, each in a different season, between August 2016 and May 2018 and covered nearly all

Deleted: Missing OH reactivity was more than 4 s^{-1} in air masses affected by pollution, althou

Deleted: gh the

Deleted: in the cleaner portions of the Mediterranean and Adriatic Seas

Formatted: Superscript

Formatted: Normal

latitudes over the Pacific and Atlantic Oceans. Although the calculated OH reactivity in the middle-to-upper troposphere is less than the OH reactivity instrument's LOD of $\sim 0.4 \text{ s}^{-1}$ at 68% confidence, this instrument can measure OH reactivity in and just above the MBL. The comprehensive instrument suite deployed aboard the NASA DC-8 airborne laboratory allows a detailed examination of which trace gases most influence measured OH reactivity.

Deleted: 1 σ

Deleted: .

2 Methods

Here we discuss the ATom campaign, the OH reactivity instrument and its measurement capabilities, the model used to generate calculated OH reactivity, and the statistical analysis that was used to find correlations with missing OH reactivity.

2.1 ATom

The ATom campaign consisted of four deployments over all four seasons, starting with Northern Hemisphere summer in 2016 and ending with Northern Hemisphere spring in 2018 (Table 1).

Deleted: n

Deleted: h

Deleted: n

Deleted: h

Each deployment used the NASA DC-8 Airborne Science Laboratory (DC-8) to profile the atmosphere by frequently ascending and descending between 0.2 km and 12 km on flights north from California to Alaska, down the Pacific to New Zealand, across the Antarctic Circle to Chile, up the Atlantic Ocean to Greenland, across the Arctic Circle to Alaska and then back to California (yellow lines in Fig. 1). As shown in Table 2, the DC-8 carried a suite of instruments that measured over 100 different chemical constituents, aerosol particle properties and chemical composition, photolysis frequencies, and meteorological variables (Wofsy et al., 2018; ATom, 2016).

2.2 OH Reactivity Measurement

The OH reactivity concept and the basic instrument have been described before for ground-based operation (Kovacs and Brune, 2001) and for aircraft operation (Mao et al., 2009). The instrument used for ATom, called OH Reactivity (OHR), is a version of the one described by Mao et al. (2009). A brief description of the concept and the instrument is presented below.

Deleted: s

Sampled air is brought into the instrument during flight by ram force at the 1.2 cm diameter inlet and the Venturi effect at the instrument outlet. A movable wand at the center of a flow tube (7.5 cm dia.) injects OH into the flow tube at different distances from an OH detection inlet and axis similar to the one used to detect OH in the atmosphere. In the wand, OH is generated in a flow of humidified carrier (N_2 or purified air), which is exposed to 185 nm radiation from a Hg lamp that photolyzes the H_2O to make OH and HO_2 . As the wand moves away from the detection axis, the signal observed of unreacted OH with the sample air decreases. Assuming a constant decay rate, measured OH reactivity is determined by Eq. (3):

$$k_{OH} = \frac{\ln\left(\frac{[OH]_0}{[OH]}\right)}{\Delta t} - k_{offset} \quad (3)$$

Deleted: background

where [OH] is the instantaneous OH concentration, [OH₀] is the initial OH concentration, Δt is reaction time between the [OH] measurements (the distance the wand moves divided by the flow speed), and k_{offset} is the instrument offset due to OH loss to the walls or to impurities in the carrier gas. The wand moves approximately 10 cm in total along its path from closest point to farthest point from the detection axis. The sampling time step is synced with the Airborne Tropospheric Hydrogen Oxides Sensor (ATHOS, an instrument used in tandem with the OHR instrument to measure in situ OH and HO₂), which samples at 5 Hz. Depending on the ATom deployment, the wand takes 15 or 20 seconds to move 10 cm and back to its starting position, where it rests for 5 or 10 seconds while the OH detection system switches the laser wavelength to off resonance with the OH absorption line to measure the signal background. Flow speeds through the OHR instrument are measured with a hot-wire anemometer and are typically between 0.25 m s⁻¹ at lower altitudes and 0.45 m s⁻¹ at higher altitudes, resulting in a typical total measured reaction time between 0.40 and 0.22 seconds.

Deleted: background

Deleted: background

Deleted: phase

Deleted: measures the background signal

Deleted: 0

It is important to note that all OH reactivity instruments measure the “instantaneous” OH reactivity, which is only the reactions that occur within the maximum reaction time observed by that instrument. This maximum time is typically less than a second. These instruments do not measure either subsequent OH reactivity or OH production if the time constants for that chemistry are greater than the maximum reaction time. In relatively clean environments, no subsequent chemistry affects the measured OH decay. However, in environments where NO is greater than a few ppbv, the reaction HO₂ + NO → OH + NO₂ is fast enough to convert HO₂ to OH, thereby altering the observed OH decay. No high NO environments were encountered in ATom.

Deleted: high NO

In all previous ground-based and aircraft-based studies, high purity N₂ was used as the carrier gas in the wand. During aircraft-based studies, a cylinder of N₂ gas was consumed on each 8-hour flight and accordingly had to be replaced before the next flight. It was not possible to position caches of N₂ cylinders at each of the ~12 layovers during each ATom phase. Instead of N₂, air from a zero-air generator (PermaPure ZA-750-12) was used as the carrier gas in the laboratory prior to ATom. Before each mission, the zero-air generator media (Perma Pure ZA-Catalyst – Palladium on Aluminum Oxide) was replaced and the air produced by the unit was verified to be pure by running it through a Potential Aerosol Mass chamber that rapidly oxidizes any VOCs to particles (Lambe et al., 2011). No particles were seen, indicating that the air had negligible amounts of larger reactive VOCs. The results of this test were consistent with those obtained by substituting the air from the zero-air generator with high purity nitrogen. The exception to this procedure was during ATom4, when the zero-air generator itself had to be replaced late in instrument integration period. The media was changed prior to the ATom4 integration and the research flights, but the air purity was unable to be checked until after the ATom4 deployment had ended, when it was found that the OHR offset was higher than in previous ATom deployments.

Deleted: phase

Deleted: background

Deleted: phases

2.3 OH Reactivity Measurement Offset Calibrations

960 The OHR offset varied between the 4 ATom deployments due to changes in the zero-air generator performance and between research flights due to internal contamination from pre-flight conditions. These changes were tracked with measurements of the OHR instrument offset in the laboratory and, for ATom4, in situ during several flights. For the laboratory calibrations, the internal pressure of the OHR instrument was varied between 30 and 100 kPa to simulate in-flight conditions. For the in situ
965 calibrations taken during the second half of ATom4, the OHR instrument was switched from sampling the ambient flow to sampling high purity N₂ from a reserve N₂ cylinder. The flow rate out of the cylinder was adjusted to match the flow speed measured by the hot-wire anemometer just prior to the switch. During ascent and descent, the internal pressure and flow speed changed too quickly over the length of one decay to get a good offset calibration, so offset calibrations were taken only from stable
970 altitude legs, predominantly at the low altitudes.

Two complete laboratory calibrations, the in situ calibration, and two calibrations only at ~100 kPa were used to determine k_{offset} for the different ATom deployments (Fig. 2). The 2017 calibration applies to ATom2 and ATom3, while the 2018 calibration applies to ATom4. For ATom1, the offset was calibrated at only 97 kPa prior to the mission, but it is in excellent agreement with the offset calibrated for ATom4. We can safely assume that the ATom4 offset slope can be applied to ATom1 because all offset calibrations performed at low OHR flowtube pressures, even those of Mao et al. (2009), are ~2 s⁻¹. The difficulty of maintaining steady calibration conditions in flight during ATom4 caused the large in situ calibration error. The standard deviation of these in situ offset calibrations is 0.75 s⁻¹, which is 2.5 to 3 times larger than the standard deviation obtained for ambient measurements in clean air for the same altitude and number of measurements, indicating that the atmospheric measurement precision is much better than could be achieved in these difficult offset calibrations. Yet even with this lower precision, the mean in situ offset at high and low pressure agree with the linear fit of the laboratory calibrations to within 20% at low pressures and 3% at high pressure. The excellent agreement between the laboratory and in situ offset calibrations for ATom4 confirms the finding of Mao et al. (2009) that laboratory offset calibrations before or after a campaign accurately capture the instrument offset during the campaign.

990 This observed pressure dependence of the offset calibration is different from the behavior of the pressure-independent offset calibration used by Mao et al. (2009). However, a re-examination of the Mao et al. (2009) data indicates that the offset during INTEX-B was also pressure dependent, with an offset of 2.9 s⁻¹ at high OHR flowtube pressure and 2.0 s⁻¹ at low OHR flowtube pressure, nearly identical to the values used for ATom2/ATom3.

995 The difference in the linear fit to the offset calibration for ATom1 and ATom4 and the linear fit to the offset calibration for ATom2 and ATom3 is pressure dependent (Fig. 2). The standard volume airflow in the wand was constant, but the ambient volume flow in the flow tube decreased by a factor of ~2, as the flow tube pressure increased from 30 kPa to 100 kPa. As a result, the contamination concentration from the wand air also increased a factor of ~2 as flow tube pressure increased. This pressure-dependent

Formatted: Heading 2

Deleted: background

Deleted: throughout the campaign due to subtle

Deleted: variations

Deleted: background

Deleted: 25

Deleted: background

Deleted: background

Deleted: background

Deleted: phases

Deleted: to ATom1 and

Formatted: Superscript

Deleted: At ~1000 hPa pressure, the standard deviation is $\pm 0.3 \text{ s}^{-1}$ for the laboratory calibrations and $\pm 0.8 \text{ s}^{-1}$ for the in situ calibrations.

Deleted: s

Deleted: r

Formatted: Superscript

Formatted: Font:(Default) +Theme Body (Times New Roman)

Formatted: Font:(Default) +Theme Body (Times New Roman)

Formatted: Font:(Default) +Theme Body (Times New Roman)

Deleted: background

Deleted: background

Deleted: background

Deleted: All calibrations are pressure-dependent, with all three background calibrations being the same to within 0.5 s^{-1} at 30 ... [2]

Deleted: background

Deleted: background

Deleted: background

Deleted: a background

Deleted: low altitudes

Deleted: high altitudes

Deleted: and

Formatted: Font:12 pt

Formatted: Font:12 pt

Formatted: Font:12 pt

Formatted: Font:12 pt

Formatted: Font:12 pt

Formatted: Font:12 pt

035 contamination concentration explains much of the difference between the two fitted lines and provides evidence that contamination in the wand flow was a substantial contributor to the changes in the zero offset between ATom1/ATom4 and ATom2/ATom3. The good agreement between the fit for ATom2/ATom3 and the offset calibrations of Mao et al. (2009), who used ultra-high purity N₂, suggests that the zero air for ATom2/ATom3 had negligible contamination.

040 The OHR instrument zero offset varied slightly from flight to flight because the variable air quality produced by the zero-air generator. This flight-to-flight variation was tracked and the OH reactivity offset was corrected by the following procedure. The OH reactivity calculated from the model at the OHR instrument's temperature and pressure (see Sect 2.3) was 0.25-0.30 s⁻¹ for the upper troposphere during all ATom deployments and latitudes. The offset calibrations were adjusted in the range of 0.34±0.32 s⁻¹ for each research flight by a pressure-invariant offset that was necessary to equate the mean measured and model-calculated OH reactivity values for data taken above 8 km altitude. If this offset correction is not used for all altitudes, then the OH reactivity in the 2-8 km range varies unreasonably from flight-to-flight, even going significantly negative at times. In effect, we used the upper troposphere as a clean standard in order to fine-tune k_{offset} just as Mao et al. (2009) did.

050 The OH signals in the upper troposphere were high enough to allow the slopes of the OH decays to be determined with good precision for each 20-30 s decay. However, at the low altitudes, quenching of the fluorescence signal by higher air and water vapor abundances reduced the OH signals. To compensate for this reduction, decays were binned into 1-minute sums before the decay slopes were calculated. Three OH signal decays from low altitudes during ATom2 are shown in Fig. 3. When k_{offset} is subtracted from the decays shown in Fig. 3, their values become ~5 s⁻¹ (blue), ~3 s⁻¹ (teal), and ~2 s⁻¹ (yellow).

2.4 Missing OH Reactivity Uncertainty Analysis

060 The uncertainty for missing OH reactivity in the MBL at the 68% confidence level comes from four components: the decay measurement itself; the offset as determined by the slope and intercepts of the fits to the laboratory OH reactivity offset calibrations (Fig. 2); the flight-to-flight offset variation as judged by fitting the measured OH reactivity to the model-calculated OH reactivity at 8-12 km altitude; and the model calculations. First, the uncertainty in decay fit is approximately ±7.5%, which for a typical OH reactivity measurement in the MBL of ~2 s⁻¹, would give an uncertainty of ±0.15 s⁻¹. Second, the uncertainty in the OH reactivity offset in the MBL is found from the sum of the slope uncertainty times the OHR flow tube pressure, which is ~100 kPa in the MBL, (±0.16 s⁻¹) and the intercept uncertainty (±0.11 s⁻¹). The two uncertainties are assumed to be correlated. Third, the uncertainty in the flight-to-flight offset variation is the standard deviation of the mean for each high altitude short level leg (±0.15 s⁻¹). Fourth, the uncertainty of the model-calculated OH reactivity was determined by Eq. 4:

$$070 \Delta k_{OH}^{calc} (s^{-1}) = \sqrt{\sum [(k_i \Delta x_i)^2 + (\Delta k_i x_i)^2]} \quad (4)$$

Deleted:
Deleted: background
Deleted: background
Deleted: phases
Deleted: Even if there was 0.3 s ⁻¹ of missing OH reactivity in the upper troposphere, this amount is below the LOD for the OHR instrument, which is ~0.4 s ⁻¹ for 1-minute sums.
Deleted: Therefore, t
Deleted: background
Deleted: 4
Deleted: make
Deleted: measured and model calculated
Deleted: OH reactivity the same near the tropopause
Deleted: background
Deleted: background
Deleted: (yellow)
Formatted: Heading 2
Formatted: Font:12 pt
Formatted: Font:12 pt
Formatted: Font:12 pt
Formatted: Font:12 pt
Formatted: Font:12 pt
Formatted: Font:12 pt
Formatted: Font:12 pt
Formatted: Font:12 pt
Formatted: Font:12 pt
Formatted: Font:12 pt
Formatted: Font:12 pt
Formatted: Font:12 pt
Formatted: Font:12 pt
Formatted: Font:12 pt
Formatted: Font:12 pt
Formatted: Font:12 pt
Formatted: Font:12 pt
Formatted: Font:12 pt
Formatted: Font:12 pt
Formatted: Font:12 pt
Formatted: Font:12 pt
Formatted: Font:12 pt
Formatted: Font:12 pt
Formatted: Font:12 pt

where k_i are the reaction rate coefficients and x_i are the OH reactant concentrations. The rate coefficient uncertainties come from Burkholder et al. (2016) and the chemical species uncertainties come from Table 2 and Brune et al. (2020). For the 11 chemical species responsible for 95% of the total OH reactivity in the MBL, this uncertainty is $\pm 0.08 \text{ s}^{-1}$. The square root of the sum of the squares of all these uncertainties yields a total uncertainty for the MBL missing OH reactivity of $\pm 0.32 \text{ s}^{-1}$ at the 68% confidence level.

The OH reactivity from the model at the ambient temperature and pressure rarely exceeded 2 s^{-1} in the planetary boundary and was only 0.2 s^{-1} in the free troposphere. These low values presented a significant challenge for our OHR instrument, as it would have for any OH reactivity instrument; even the most precise instrument measuring in a chamber at its home laboratory has a LOD of $\pm 0.2 \text{ s}^{-1}$, 68% confidence, for a measurement integration time of 60-160 seconds (Fuchs et al., 2017). If the same instrument were to sample air masses on an aircraft traveling 200 m s^{-1} , its precision would likely be degraded. From this perspective, the LOD on these ATom measurements is about as low as that for any other OH reactivity measurements.

The analysis in the paper is focused on the first three ATom phases. ATom4 is excluded from this analysis for two reasons. First, offset calibrations were performed during more than half of the low-altitude periods over the Atlantic, severely limiting the ambient measurements in the MBL. Second, the increased contamination during ATom4 made the OH reactivity measurements 2-3 times noisier than during the previous ATom deployments.

2.5. Photochemical Box Model

The photochemical box model used to calculate OH reactivity is the Framework for 0-D Atmospheric Modeling (F0AM) (Wolfe et al, 2016). It uses the Master Chemical Mechanism v3.3.1 (MCMv331) for all gas-phase reactions (Jenkin et al., 1997; Saunders et al., 2003). Both the F0AM model framework and MCMv3.3.1 are publicly available. The reactions of $\text{CH}_3\text{O}_2 + \text{OH}$ and $\text{C}_2\text{H}_5\text{O}_2 + \text{OH}$ were added to the model mechanism with rate coefficients from Assaf et al. (2017). The model was run with the integration time set to 3 days with a first-order dilution lifetime of 12 hours, although the calculated OH reactivity was the same to within a few percent for an order-of-magnitude change in these times. The model was constrained by the simultaneous measurements listed in Table 2. These measurements were taken from the 1-second merge file, averaged to 1-minute values, and interpolated to a common 1-minute time step. In cases where multiple measurements of a chemical species exist (e.g., CO), a primary measurement was chosen and other measurements were used to fill gaps in the primary measurement.

To compare measured and calculated OH reactivity, the model-calculated OH reactivity must be corrected to the OHR flow tube pressure and temperature. For the rest of this paper, "calculated OH reactivity" will refer to these corrected values. Equation 1 was used to find the calculated OH reactivity. If the measured and calculated OH reactivity agreed, then there was no missing OH reactivity to within

Formatted: Font:12 pt

Formatted: Font:12 pt

Formatted: Font:12 pt

Formatted: Font:12 pt

Formatted: Font:12 pt

Formatted: Font:12 pt

Deleted: ... [3]

Formatted: Font:(Default) +Theme Body (Times New Roman)

Formatted: Font:12 pt

Formatted: Font:(Default) +Theme Body (Times New Roman), 12 pt

Formatted: Font:(Default) +Theme Body (Times New Roman)

Deleted: Therefore, in each ATom phase, the total uncertainty in the OH reactivity is dominated by the instrument background uncertainty.

Deleted: calculated

Deleted: 1σ

Deleted: background

Deleted: phases

Deleted: 3

Deleted:

Deleted: The OHR flow tube temperature and pressure were used to calculate reaction rate coefficients and reactant concentrations to compare with the observations

Deleted: then

Deleted: model

the uncertainties for both the measured and the calculated values. However, if there was missing OH reactivity in the flow tube, then the missing OH reactivity in the atmosphere may be different because the temperature dependence of its reaction rate coefficients is unknown. Fortunately, the focus of this study is in and just above the MBL where the flow tube pressures and temperatures are nearly identical to atmospheric temperatures and pressures. The OH reactivity calculated from the model output at the flow tube pressure and temperature is within $\pm 10\%$ of that calculated at ambient conditions. Thus, the missing OH reactivity at the flow tube temperature and pressure is assumed to be equal the atmospheric missing OH reactivity.

Deleted: model

Formatted: Font:12 pt

Deleted: Thus, the missing OH reactivity calculated at flow tube temperature and pressure is assumed to be equal the atmospheric missing OH reactivity.

If missing OH reactivity is found, a likely source is unknown VOCs or OVOCs, which we will call X. The abundance of X was determined from the missing OH reactivity by Eq. (5).

$$X = \frac{mOHR}{k_{X+OH}} \frac{10^9}{M} \quad (5)$$

where X is the missing chemical species (ppbv), $mOHR$ is the missing OH reactivity, k_{X+OH} is the reaction rate coefficient for the reaction $X + OH \rightarrow$ products, and M is the air number concentration. We assume that $k_{X+OH} = 10^{-10} \text{ cm}^3 \text{ s}^{-1}$, which gives X a lifetime of about an hour for the typical daytime $[OH]$ of $\sim 3 \times 10^6 \text{ cm}^{-3}$. For these assumptions, an X abundance of 400 pptv corresponds to a missing OH reactivity of 1 s^{-1} . This arbitrary rate coefficient approximates a rate coefficient for a reaction of a sesquiterpene with OH. If X is an alkane or alkene that has a lower reaction rate coefficient, then the required X abundance would be larger.

Formatted: Font:Italic

Formatted: Font:Italic

Formatted: Superscript

Simple X oxidation chemistry was added to the photochemical mechanism to test the impact of X on the modeled OH and HO_2 . This assumed additional chemistry is provided in Table 3. XO_2 is used to designate the peroxy radical formed from X . Rate coefficients for CH_3O_2 and CH_3OOH were assumed to apply to XO_2 and XOOH . Case 1 assumes that no OH is regenerated in the oxidation sequence for X , while case 2 assumes that OH is regenerated for every oxidation sequence of X .

2.6 Correlation Analysis

Deleted: 5

An analysis of correlations between missing OH reactivity and the chemical or environmental factors could indicate possible causes of the missing OH reactivity. Linear regressions were found for missing OH reactivity and every measured and model-calculated chemical species and meteorological parameter. Model-calculated chemical species with abundances less than 1 pptv were not included in the regressions. SST and chlorophyll data come from NASA Earth Observations (2019). Correlations were performed on the first three ATom deployments individually and the first three ATom deployments combined.

Deleted: If missing OH reactivity persists after the background is subtracted from the OH reactivity measurements and a comparison is made to the model calculated OH reactivity, then a correlation analysis might determine its causes, which could then be further investigated.

Moved (insertion) [1]

Deleted: phases

Deleted: phases

To reduce the noise in the missing OH reactivity values prior to doing any correlation analysis, the 1-minute missing OH reactivity values were averaged into "per-dip" bins and "per-flight" bins. The term "per-dip" means that the missing OH reactivity was averaged over each dip, typically a 5-minute level-

Deleted: summed

195 altitude leg at 160 m. The term “per-flight” means that the missing OH reactivity for all the dips in a flight were averaged together. The standard deviation of the 1-minute measurements within each dip was typically 0.4 s^{-1} , while the standard deviation of the per-dip measurements in a flight was 0.25 s^{-1} . The low-level legs used for the per-dip means were generally in the MBL because its height was greater than 160 m 85% of the time. The MBL height is the altitude below which the potential temperature is constant. Each per-flight bin is the mean of each flight’s per-dip set. A per-dip bin occurred roughly every hour of flight. Each per-flight bin spanned only a few degrees of latitude near the poles but as much as 50° of latitude in the tropics. Only the measurements made while flying over the ocean were included in the per-dip and per-flight averaging because the dips over land sampled terrestrial or ice emissions and not ocean emissions.

200
205 Individual measured or calculated meteorological parameters and chemical species passed a preliminary correlation threshold for missing OH reactivity if the sign of each regression was the same for ATom1, ATom2, and ATom3. Correlations that passed this preliminary filter had their R^2 values averaged between each deployment individually and grouped together. The averaged correlation coefficients were then tallied and ranked from greatest to least R^2 . The top 10% of these correlations for both the per-dip and per-flight averages were combined into one data set. Because the missing OH reactivity showed some latitude dependence, the same multi-step technique was performed on all the chemical species and meteorological parameters in different hemispheres: Northern, Southern, Eastern, and Western. Both data sets were then combined into a single data set and the strongest of these correlations were reported.

3 Results

220 The focus of these results is the OH reactivity measurements in and just above the MBL. However, the OH reactivity measurements are shown for the entire range of altitudes, even though the high-altitude ($>8 \text{ km}$) OH reactivity values were set to the model calculated OH reactivity that was corrected to the OHR flow tube pressure and temperature.

3.1 Global OH Reactivity Versus Altitude

225 The average calculated global OH reactivity at the lowest altitudes is about an order of magnitude less than the average OH reactivity in cities or forests (Yang et al., 2016), which is typically $10\text{-}50 \text{ s}^{-1}$. Model-calculated OH reactivity is less than 2 s^{-1} averaged over all latitudes and seasons (Fig. 4). In different seasons and regions, this calculated OH reactivity consists of CO (30-40%), CH_4 (19-24%), methyl hydroperoxide (MHP) (5-16%), aldehydes (11-12%), H_2 (6-7%), O_3 (2-5%), and HO_2 (2-6%), H_2O_2 (0-5%), and CH_3O_2 (0-7%) with the remaining reactants totaling less than 10%. The ordering of these reactants is similar to that of Mao et al. (2009), although in their work the calculated OH reactivity due to CO was about 60% and CH_4 about 15%, and all OVOCs about 16%. Part of this difference can be ascribed to more OVOC measurements in ATom and the greater CO abundances in the Northern Hemisphere where INTEX-B occurred.

Deleted: 5
Deleted: Each per-dip bin is a single value representing an average of the missing OH reactivity as the DC-8 flew a level leg at 200 m.
Deleted: se
Deleted:
Deleted: all
Deleted: greater than 200 m
Deleted: average
Deleted: and is an average of ~5 minutes of missing OH reactivity values
Deleted: points
Deleted: taken
Deleted: as
Formatted: Font:12 pt

Deleted: Individual measured or model calculated meteorological parameters or chemical species passed a preliminary correlation threshold for missing OH reactivity if the sign of each regression was the same for ATom1, ATom2, and ATom3. Correlations that passed this preliminary filter had their R^2 values averaged between each phase individually and grouped together. Some extreme outlier points were removed before correlations were calculated. The averaged correlation coefficients were then tallied and ranked from greatest to least R^2 . The top 10% of these correlations for both the per-dip and per-flight averages were combined into one list. The same multi-step technique was performed on all the chemical species and meteorological parameters as they were correlated with latitude as well, under a similar breakdown for Northern, Southern, Eastern and Western hemispheres. Both lists were then combined into a single list and the strongest of these correlations were reported.

Formatted: Space After: 12 pt, Line spacing: single

Deleted: 10

Deleted: The average calculated global OH reactivity at the lowest altitudes is about an order of magnitude less than the average OH reactivity in cities or forests (Yang et al., 2016). Model-calculated OH reactivity is less than 2 s^{-1} averaged over all latitudes and seasons (Fig. 4). In different seasons and regions, this calculated OH reactivity consists of CO (30-40%), CH_4 (19-24%), methyl hydroperoxide (MHP) (5-16%), aldehydes (11-12%), H_2 (6-7%), O_3 (2-5%), and HO_2 (2-6%), with the remaining reactants totaling less than 10%. The ordering of these reactants is similar to that of Mao et al. (2009), although in their work the calculated OH reactivity due to CO was about 60% and CH_4 about 15%, and all OVOCs about 16%. Part of this difference can be ascribed to more OVOC measurements in ATom and the greater CO abundances in the Northern hemisphere where INTEX-B occurred.

Deleted: Over Oceans

Formatted: Superscript

The calculated OH reactivity decreases from $\sim 1.5 \text{ s}^{-1}$ in the MBL to $0.25\text{-}0.30 \text{ s}^{-1}$ in the upper troposphere (Fig. 4). The mean measured OH reactivity has been matched to the mean calculated OH reactivity for altitudes above 8 km, but the two are independent at lower altitudes. The mean measured and calculated OH reactivity agree to within combined uncertainties for altitudes between 8 km and 2-4 km, but the mean measured OH reactivity becomes increasingly greater than the mean calculated below 2-4 km and especially in the MBL. However, the differences in the mean values is not the best way to understand these differences between measured and calculated OH reactivity.

Formatted: Superscript

Formatted: Superscript

3.2 Missing OH Reactivity: Statistical Evidence

A better approach is to find the missing OH reactivity for each measurement point and then compare the mean values. The missing OH reactivity is plotted as a function of altitude for ATom1, ATom2, and ATom3 (Fig. 5). The mean missing OH reactivity is set to 0 s^{-1} for 8-12 km, but remains near to 0 from 8 to 2-4 km, where it increases. The 1-minute measurements are a good indicator of the measurement precision, which is $\pm 0.35 \text{ s}^{-1}$ for ATom1 and $\pm 0.25 \text{ s}^{-1}$ for ATom2 and ATom3.

Deleted: The median measured OH reactivity equals the median model-calculated OH reactivity to within $\pm 1\sigma$ statistical uncertainty until below 2-4 km, where it becomes greater than the median model-calculated OH reactivity (Fig. 4). The median missing OH reactivity becomes greater than 0 below 2-4 km, depending on the ATom phase, reaching median values between 0.2 and 0.8 s^{-1} in the marine boundary layer (MBL) for ATom1 through ATom3. In some locations, primarily the northern and tropical Pacific Ocean, missing OH reactivity was $1\text{-}2 \text{ s}^{-1}$, and even larger on a few occasions.

Formatted: Superscript

In the MBL, the mean missing OH reactivity is 0.4 s^{-1} for ATom1, 0.5 s^{-1} for ATom3, 0.7 s^{-1} for ATom2. From a Student t-test in which the MBL missing OH reactivity is compared to either the values at 6-8 km or 8-12 km altitude ranges, the differences in mean missing OH reactivity between the MBL and the higher altitudes is statistically significant for a significance level, α , equal to 0.01, with p-values $< 10^{-15}$. However, the mean MBL missing OH reactivity values are close to the upper limit on the absolute missing OH reactivity uncertainty (95% confidence), which is 0.64 s^{-1} (blue bar, Fig. 5). There is a small probability (2-10%) that the mean MBL missing OH reactivity is due only to absolute error in the missing OH reactivity measurement that was derived in Section 2.4.

Formatted: Superscript

Formatted: Superscript

The mean MBL missing OH reactivity contains measurements for which the missing OH reactivity is 0 s^{-1} . The real interest is in the missing OH reactivity that is greater than can be explained by absolute missing OH reactivity measurement error or precision. From Fig 5, it is clear that the positive scatter of data is much greater than the negative. The means of standard deviations of the negative values and of the positive values were calculated for 1-km height intervals (dashed lines). These lines and the individual data points both indicate skewness in the missing OH reactivity, especially in the lowest 2-4 km altitude. A skewness test shows that, in and just above the MBL, missing OH reactivity from ATom1 and ATom2 exhibit weak-to-moderate skewness (~ 0.4) in the MBL while missing OH reactivity from ATom2 exhibits strong skewness (1.4).

Formatted: Superscript

Formatted: Superscript

Deleted: For missing OH reactivity to be meaningful, some missing OH reactivity points must be much greater than the statistical spread of the OH reactivity measurements. Missing OH reactivity is not measured above 8 km because we assumed no measurable OH reactivity was there in order to identify the internal instrument contamination for each flight. However, these data provide insight into the measurement precision (Fig. 5). Missing OH reactivity is shown for ATom1, ATom2, and ATom3. The dotted black bands represent $\pm 2\sigma$ standard deviation for data averaged into 0.5 km altitude bins. About 95% of all points above 4 km are within that phase's 2σ uncertainty bands, which is consistent with a statistically normal distribution.

Formatted: Superscript

Quantile-quantile plots (Q-Q plots) provide a visual description of the relationship between a sample distribution and a normal distribution. The standard normal quantiles are plotted on the x-axis and the sample quantiles on the y-axis. If the sample is perfectly normally distributed, then its values will lie along a straight line. Data lying higher than the line for values on the right side of the normal distribution (positive standard normal quantiles) indicate more high-value data than expected, while

Deleted: of the differences in the distributions of missing OH reactivity values above 8 km and below 4 km, representing the top third (8-12 km) and bottom third (0-4 km) of the sampled troposphere (Fig. 6).

data higher than the line for values on the left side of the normal distribution (negative standard normal quantiles) indicate fewer low-value data than expected.

345 Q-Q plots are shown for three ATom2 cases in Fig. 6. The large boxes are the interquartile range
between the 1st quartile (25% of the data below it) to the 3rd quartile (75% below). The missing OH
350 reactivity data for altitudes greater than 8 km (red data) is normally distributed until the standard normal
quantile of 2, meaning that less than a few percent of the data is higher than expected. On the other
hand, the missing OH reactivity data in the MBL (blue data) are normally distributed between standard
355 normal quantiles of -2 and 1, meaning that a few percent of low-value are less than expected, but, more
importantly, as much as 20% of the high-value data is greater than expected. Also included in Fig. 6 is
the case for which we assume that the MBL missing OH reactivity zero value is actually greater by the
missing OH reactivity absolute uncertainty at 95% confidence (gray data). Comparing these two MBL
cases shows that changes in the mean missing OH reactivity values affect only the median value and not
the distribution skewness. Q-Q plots for ATom1 and ATom2 (not shown) are less dramatic, but still
have the same characteristics: for measurements above 8 km, the high-value data are more normally
distributed; for the MBL, ~20% of high-value data are greater than expected.

360 All of these statistical tests provide strong evidence for an abnormal amount of larger-than-expected
missing OH reactivity in the MBL and up to 2-4 km altitude. It is possible that some individual outliers
of the 1-minute data are due to anomalous OHR instrument issues. The few outlier data points at higher
altitude could be due to these instrument issues but may also be due to pollution plumes that were
encountered. However, it seems highly unlikely that ~20% of the higher-than-expected data at low
365 altitudes could be caused by them. Thus, OH reactivity in the MBL is likely missing and needs to be
further investigated.

3.3 Global Missing OH Reactivity in the Marine Boundary Layer

370 The frequent dips to below 200 m altitude gave more than 100 opportunities to examine the global
distribution of missing OH reactivity. The measured OH reactivity averaged for each dip (Fig. 7(a, c, d)
in the MBL (filled circles) is generally greater in the mid-latitudes and tropics than in the higher
latitudes, reaching as high as $4\text{--}5 \text{ s}^{-1}$ over the Northern Hemisphere Pacific Ocean. More typical
calculated values are $1.5 \pm 0.6 \text{ s}^{-1}$, with relatively little variation. As a result, the missing OH reactivity
values reflect the measured OH reactivity values.

375 Missing OH reactivity varied from $\sim 0 \text{ s}^{-1}$ to $\sim 2.5 \text{ s}^{-1}$ (Fig. 7 (b, d, f)). The lowest values occurred
predominantly in the polar regions but also occasionally in the mid-latitudes and tropics. High values
exceeding 1 s^{-1} occurred predominantly over the Northern Hemisphere Pacific Ocean. The highest
values occurred in ATom2, but values exceeding 2 s^{-1} were also observed in ATom3. Missing OH
380 reactivity appears to vary in both place and time.

Deleted:

Deleted: If these values were purely normal distributions, as would be expected from a missing OH reactivity created solely by the instrument uncertainty, then they would lie along the red dashed lines. Values higher than the red dashed line indicate that the number of missing OH reactivity values in that part of the distribution is much greater than would be expected for a normal distribution. The missing OH reactivity values measured below 4 km altitude lie along the red dashed line, which passes through (0.0, 0.0), indicating that the median value is 0 s^{-1} and the values follow the normal distribution. However, while more than 90% of the missing OH reactivity values below 4 km follow the normal distribution, there are many missing OH reactivity values that fall above those predicted by a strictly normal distribution. This deviation from a normal distribution indicates that the missing OH reactivity exceeds the statistical error range. ... [4]

Formatted: Normal

Formatted: English (UK), Superscript

Formatted: English (UK), Superscript

Formatted: English (UK), Superscript

Formatted: English (UK), Superscript

Formatted: English (UK), Superscript

Formatted: English (UK), Superscript

A plot of missing OH reactivity as a function of latitude shows these variations in place and time (Fig. 8). There is a general tendency for missing OH reactivity to be greatest over the mid-latitudes and tropics and to decrease toward the poles. A sampling bias (Fig. 7) may be the reason for near-zero missing OH reactivity in the northern high latitudes and not in the southern high latitudes. However, the high missing OH reactivity over the Northern Hemisphere Pacific Ocean is exceptional.

A special note should be made regarding the northern Pacific data for ATom2. One flight (Anchorage, Alaska to Kailua-Kona, Hawai'i) accounts for missing OH reactivity values greater than $\sim 2.5 \text{ s}^{-1}$. These points are anomalous in the context of all ATom OH reactivity measurements, and they do not correlate with the modeled influence from fires, convection, land, or the stratosphere. While present on all figures except Fig. 8, they were not included in the correlation analysis described below.

3.4 OH Reactivity Over Land

Of the approximately 120 dips in which OH reactivity measurements were made, 14% were over land (Figure 7). The majority of these were made in the Arctic, several over snow, ice, and tundra. As a result, the mean calculated OH reactivity was only 1.35 s^{-1} , while the mean measured OH reactivity was 1.4 s^{-1} and the mean missing OH reactivity was -0.1 s^{-1} , which is essentially zero to well within uncertainties. Note, however, that there is little missing OH reactivity over most of the Arctic polar oceans as well as over the Arctic land, which means that missing OH reactivity is generally low over the entire colder Arctic region. The greatest measured missing OH reactivity was found on only one dip over the Azores, where the missing OH reactivity was $\sim 2.5 \text{ s}^{-1}$ larger than the calculated OH reactivity.

3.5 Correlation of Missing OH Reactivity with Other Factors

From the procedure given in Section 2.6, missing OH reactivity has the four strongest correlations with butanal ($\text{C}_3\text{H}_7\text{CHO}$), dimethyl sulfide (DMS, CH_3SCH_3), formaldehyde (HCHO), and sea surface temperature (SST), as shown in Fig. 9. Missing OH reactivity also correlates with some modeled pptv-level butanal products, but at these low levels, these chemical species could not be the source of the missing OH reactivity. Interestingly, missing OH reactivity correlates only weakly with acetaldehyde and chlorophyll. These correlations suggest that the missing OH reactivity comes from an unknown VOC or OVOC that has HCHO and butanal as products and is co-emitted with DMS. The correlation with SST suggests an ocean source, as a higher temperature implies more emissions. Either biological activity of phytoplankton in the sea surface microlayer (Brooks and Thornton, 2017; Lana et al., 2011) or abiotic sea surface interfacial photochemistry (Brüggenmann et al., 2018) could be the source of these VOCs and OVOCs.

3.6 Comparison to INTEX-B

HCHO is a good indicator for VOC photochemistry because it is an oxidation product for many VOCs.

Formatted: Normal, No widow/orphan control

Formatted: Normal

Formatted: Superscript

Formatted: Superscript

Formatted: Superscript

Formatted: Heading 2, Widow/Orphan control

Deleted: 3

Deleted: -

A special note should be made regarding the northern Pacific data for ATom2. One flight (Anchorage, Alaska to Kailua-Kona, Hawai'i) accounts for every missing OH reactivity value greater than $\sim 2 \text{ s}^{-1}$. These points are anomalous in the context of all ATom OH reactivity measurements, and they do not correlate with the modeled influence from fires, convection, land, or the stratosphere. While present on some figures for completeness, they were not included in the correlation analysis. -

Deleted: A special note should be made regarding the northern Pacific data for ATom2. One flight (Anchorage, Alaska to Kailua-Kona, Hawai'i) accounts for every missing OH reactivity value greater than $\sim 2 \text{ s}^{-1}$. These points are anomalous in the context of all ATom OH reactivity measurements, and they do not correlate with the modeled influence from fires, convection, land, or the stratosphere. While present on some figures for completeness, they were not included in the correlation analysis. -

Deleted: Following

Deleted: 5

Deleted: the main correlations that stand out are

Deleted: 8

Deleted: A number of

Deleted:

Deleted: also correlate with missing OH reactivity

Moved up [1]: SST and chlorophyll data come from NASA Earth Observations (2019).

Deleted: 4

Thus, HCHO should correlate with missing OH reactivity. The ATom missing OH reactivity at the per-dip time resolution is compared to [the Mao et al. \(2009\)](#) missing OH reactivity below 2 km for times when NO is less than 100 pptv (Fig. 9). We use the per-dip time resolution of ~5 minutes in this comparison rather than per-flight to better align with the time resolution in Mao et al. (2009) of 3.5 minutes. [The anomalously high missing OH reactivity from ATom2 are not included in the data for the linear fit.](#) The INTEX-B correlation coefficient between missing OH reactivity and HCHO ($R^2 = 0.58$) is [better](#) than the one found for ATom ($R^2 = 0.35$), [but](#) in the range of ATom HCHO (100 pptv – 500 pptv), the ATom [correlation coefficient is larger](#).

[The linear fit of the missing OH reactivity against HCHO data from Mao et al. \(2009\) is given as the solid red line in Fig. 9. If instead the pressure-dependent offset is used for Mao et al. \(2009\), then the resulting missing OH reactivity against HCHO follows the dashed red line. With the absolute INTEX-B offset uncertainty at \$\pm 0.5 \text{ s}^{-1}\$ and the absolute ATom offset uncertainty at \$\pm 0.32 \text{ s}^{-1}\$, both at the 68% confidence level, the linear fits for missing OH reactivity against HCHO in ATom and INTEX-B agree to within combined uncertainties. The ATom linear fit slope is only 2.7 standard deviations from the INTEX-B slope, but is 4.4 standard deviations from a line with zero slope, making it highly unlikely that missing OH reactivity is not correlated with HCHO. The INTEX-B and ATom slopes to the linear fits are not exactly the same. However, given the uncertainties, the HCHO dependence of the adjusted missing OH reactivity found in INTEX-B is consistent with that found for the ATom missing OH reactivity over the northern Pacific Ocean.](#)

4 Discussion

Mao et al. (2009) calculated HO_2/OH assuming that the cycling between OH and HO_2 was much greater than HO_x production. That assumption is not valid for ATom because the low NO and OH reactivity values reduce the recycling to rates comparable to HO_x production ([Brune et al., 2020](#)). On the other hand, by adding simple X photochemistry to the MCMv331 mechanism, as discussed in Section 2.3, it is possible to determine if the measured OH and HO_2 are consistent with observed missing OH reactivity. For case 1 in which there is no OH produced in the X oxidation sequence, the modeled OH and HO_2 become [30-40% less](#) than observed at altitudes below 2 km. On the other hand, if XO_2 and its products autoxidize to produce OH (Crouse et al., 2013), then the modeled OH [and](#) HO_2 become [10-20% greater](#) than observed. The optimum agreement between observed and modeled OH and HO_2 would require a partial recycling of OH, but without knowing the identity of X, it is not possible to know the fraction of OH that should be recycled in the chemical mechanism. Thus, this analysis neither supports nor refutes the missing OH reactivity measurements.

Several recent studies provide evidence for an unknown VOC or OVOC emitted into the atmosphere from the ocean. Oceanic sources have also been proposed for butanes and pentanes in some regions (Pozer et al., 2010) and for methanol (Read et al., 2012). Measurements of biogenic VOCs in coastal waters found monoterpenes, C12-C15 n-alkanes, and several higher aldehydes that could contribute to enhanced OH reactivity (Tokarek et al., 2019).

Deleted: 's

Formatted: Font:12 pt

Deleted: While the overall

Deleted: greater

Deleted: case is better correlated

Deleted: The ATom results corroborate the Mao et al. correlation of missing OH reactivity with HCHO.

Formatted: Font:12 pt

Deleted: The linear fit of the missing OH reactivity against HCHO data from Mao et al. (2009) is given as the solid red line in Fig. 9. If instead the pressure-dependent background is used, then the resulting missing OH reactivity against HCHO follows the dashed red line. With the INTEX-B background uncertainty at $\pm 0.5 \text{ s}^{-1}$ and ATom background uncertainty at $\pm 0.4 \text{ s}^{-1}$, both at the 1 σ confidence level, the linear fits for missing OH reactivity against HCHO in ATom and INTEX-B agree to within combined uncertainties. Thus, the adjusted missing OH reactivity found in INTEX-B is consistent with the missing OH reactivity found in the ATom phases over the northern Pacific Ocean.

Deleted: substantially less

Deleted: 6

Deleted: and to a lesser extent

Deleted: greater

Deleted: e

525 Unexpectedly large abundances of acetaldehyde (CH_3CHO) have been observed in the marine boundary layer and the free troposphere (Singh et al., 2004; Millet et al., 2010; Read et al., 2012; Nicely et al., 2016; Wang et al., 2019) and the ocean is suspected to be the source. While earlier measurements may have been compromised with interferences, recent measurements of unexpectedly large acetaldehyde abundances are supported by unexpectedly large abundances of peroxyacetic acid, which is produced almost exclusively through acetaldehyde oxidation (Wang et al., 2019). Wang et al. observed that the ocean effects on acetaldehyde were confined primarily to the MBL and were able to approximately model the vertical distribution by using direct ocean emissions of acetaldehyde. However, it is possible that some of the observed acetaldehyde was produced by rapid oxidation of VOCs or OVOCs emitted from the ocean.

Deleted: high

535 The missing OH reactivity is primarily in the MBL, but often extends upward to as high as 2 km to 4 km in some dips. Above 4 km, the OH reactivity measurements are too near their LOD and thus too noisy to know if missing OH reactivity and acetaldehyde decrease the same way with altitude, but it is possible that they do. A similar decrease with altitude would imply that the unknown reactant lives long enough to be distributed throughout the free troposphere. If, on the other hand, the missing OH reactivity is only in and just above the planetary boundary layer, then the unknown reactant could have a much shorter lifetime. The lack of correlation between missing OH reactivity and acetaldehyde in the MBL suggests that the unknown reactant responsible for the missing OH reactivity is not necessarily connected only to an ocean source of acetaldehyde.

545 From Eq. (5) and the measured missing OH reactivity, the abundance of the chemical species X would typically be a few tenths of a ppbv, assuming that X is a sesquiterpene with a typical reaction rate coefficient of $1 \times 10^{-10} \text{ cm}^3 \text{ s}^{-1}$. The mean value for X is 0.26 ± 0.23 ppbv for the per-dip bins. If X is an alkane with a typical reaction rate coefficient of $2.3 \times 10^{-12} \text{ cm}^3 \text{ s}^{-1}$, then its mixing ratio would need to be more than 10 ppbv.

Deleted: di

550 If the unknown VOC is an alkane with a reaction rate coefficient with OH of $2.3 \times 10^{-12} \text{ cm}^3 \text{ s}^{-1}$, then an unlikely large oceanic source of 340 Tg C yr^{-1} would be necessary (Travis et al., 2020). Adding this much additional VOC reduces global modeled OH 20-50% along the flight tracks, degrading the reasonable agreement with measured OH. Large sources of long-lived unknown VOCs, which do not have as large an impact on modeled OH, are also necessary to reduce but not resolve the discrepancies between measured and modeled acetaldehyde, especially in the Northern Hemisphere summer. These issues between a global model and measured missing OH reactivity and acetaldehyde need to be resolved.

Formatted: Font:12 pt

Formatted: Font:12 pt

Deleted: The lifetime of the unknown VOC is important because it determines the source strength necessary to maintain the measured missing OH reactivity. For instance, if the unknown VOC is an alkane with a reaction rate coefficient with OH of $2.3 \times 10^{-12} \text{ cm}^3 \text{ s}^{-1}$, then an unlikely large oceanic source of 360 Tg C yr^{-1} would be necessary (Travis et al., 2019). However, if the unknown VOC is an alkene, such as a sesquiterpene, then the reaction rate coefficient with OH would be $\sim 1 \times 10^{-10} \text{ cm}^3 \text{ s}^{-1}$ and the required oceanic source would be a more reasonable 8 Tg C yr^{-1} .

5 Conclusion

560 Measured OH reactivity significantly exceeds calculated OH reactivity in the marine boundary layer during ATom. This missing OH is most prominent over the northern and tropical Pacific Ocean where it

575 had mean values of $0.4\text{--}0.7\text{ s}^{-1}$ for the different ATom phases, but rose to more than 2 s^{-1} in some
locations. These higher values correspond to ~ 0.26 ppbv of a fast-reacting VOC, such as a
sesquiterpene. The correlation of missing OH reactivity with formaldehyde, butanal, dimethyl sulfide,
and sea surface temperature and the requirements for a smaller unknown reactive gas abundance and
ocean source strength suggest that an ocean source of short-lived reactive gases, possibly VOCs or
OVOCs, is responsible. This missing OH reactivity is qualitatively consistent with the observed
580 unexpectedly large abundances of acetaldehyde, peroxyacetic acid, and other oxygenated VOCs. They
may share the same cause. Finding this cause will require focused studies of detailed atmospheric
composition in regions where missing OH reactivity and acetaldehyde excess are greatest.

Deleted: di
Deleted: 2
Deleted: 8
Formatted: Superscript
Deleted: 1-
Deleted: 5

Data and Model Availability

The data and model used in this paper are publicly available:

- data: <https://doi.org/10.3334/ORNLDAAAC/1581>
- model framework: <https://github.com/airchem/F0AM>
- MCMv331 chemical mechanism: <http://mcm.leeds.ac.uk/MCM/>

Author Contribution

590 ABT, DOM, and WHB made the OH, HO₂, and OH reactivity measurements, performed the model runs, analyzed the data,
and wrote the manuscript. GMW provided support of the use of the F0AM model framework used for the model runs. WHB,
DOM, ABT, HMA, DRB, TPB, RC, JDC, BCD, GSD, JPD, JWE, SRH, TFH, RAH, EH, MJK, KM, FLM, JMN, JP, TBR,
JMS, CS., APT, CT, KU, POW, GMW provided ATom measurements used for the modeling and reviewed and edited the
manuscript.

Competing Interests

The authors declare no financial or affiliation conflicts-of-interest.

595 Funding

This study was supported by the NASA grant NNX15AG59A. This material is based upon work
supported by the National Center for Atmospheric Research, which is a major facility sponsored by the
National Science Foundation under Cooperative Agreement No. 1852977.

Acknowledgements

600 The authors thank the NASA ATom management team, pilots, logistical support team, aircraft operations team, and fellow
scientists. [We thank the reviewers for their helpful comments on the initial submission.](#)

References

605 Apel, E. C., Hornbrook, R. S., Hills, A. J., Blake, N. J., Barth, M. C., Weinheimer, A., Cantrell, C., Rutledge, S. A., Basarab,
B., Crawford, J., Diskin, G., Homeyer, C. R., Campos, T., Flocke, F., Fried, A., Blake, D. R., Brune, W., Pollack, I.,
Peischl, J., Ryerson, T., Wennberg, P. O., Crouse, J. D., Wisthaler, A., Mikoviny, T., Huey, G., Heikes, B.,
O'Sullivan, D., and Riemer, D. D.: Upper tropospheric ozone production from lightning NO_x-impacted convection:
Smoke ingestion case study from the DC3 campaign, *J. Geophys. Res. Atmos.*, doi:10.1002/2014JD022121, 2015.

Deleted: Journal of Geophysical Research: Atmospheres
Formatted: Font:Not Italic

- 615 Assaf, E., Sheps, L., Whalley, L., Heard, D., Tomas, A., Schoemaeker, C., Fittschen, C.: The Reaction between CH₃O₂ and OH Radicals: Product Yields and Atmospheric Implications, *Environ. Sci. Technol.*, 51, 2170–2177, DOI: 10.1021/acs.est.6b06265, 2017.
- ATom: Measurements and modeling results from the NASA Atmospheric Tomography Mission, available at: <https://espoarchive.nasa.gov/archive/browse/atom> (last access: 9 August 2019), 2016.
- 620 Brooks S.D., Thornton D.C.O.: Marine Aerosols and Clouds, *Annual Review of Marine Science*, 10, 289-313, <https://doi.org/10.1146/annurev-marine-121916-063148>, 2017.
- Brüggemann, M., Hayeck, N., George, C.: Interfacial photochemistry at the ocean surface is a global source of organic vapors and aerosols, *Nature Communications*, 9, Article number: 3222, 2018.
- 625 **Brune, W. H., Miller, D. O., Thames, A. B., Allen, H. M., Apel, E. C., Blake, D. R., et al.: Exploring oxidation in the remote free troposphere: Insights from Atmospheric Tomography (ATom), *J. Geophys. Res., Atmos.*, 125, e2019JD031685, <https://doi.org/10.1029/2019JD031685>, 2020.**
- Cazorla, M., Wolfe, G. M., Bailey, S. A., Swanson, A. K., Arkinson, H. L., and Hanisco, T. F.: A new airborne laser-induced fluorescence instrument for in situ detection of formaldehyde throughout the troposphere and lower stratosphere. *Atmos. Meas. Tech.*, 8, 541-552. doi:194-10.5194/amt-8-541-2015, 2015.
- 630 Chan, K. R., Dean-Day, J., Bowen, S. W., and Bui, T. P.: Turbulence measurements by the DC-8 meteorological measurement system. *Geophys. Res. Lett.*, 25, 1355-1358. doi: 10.1029/97GL03590, 1998.
- Chen, H., Karion, A., Rella, C. W., Winderlich, J., Gerbig, C., Filges, A., Tans, P. P.: Accurate measurements of carbon monoxide in humid air using the cavity ring-down spectroscopy (CRDS) technique. *Atmos. Meas. Tech.*, 6, 1031-1040. doi: 10.5194/amt-6-1031-2013, 2013.
- 635 Colman, J. J., Swanson, A. L., Meinardi, S., Sive, B. C., Blake, D. R., and Rowland, F. S.: Description of the analysis of a wide range of volatile organic compounds in whole air samples collected during PEM-Tropics A and B. *Anal. Chem.*, 73, 3723-3731. doi: 10.1021/ac010027g, 2001.
- Crouse, J. D., McKinney, K. A., Kwan, A. J., and Wennberg, P. O.: Measurement of gas-phase hydroperoxides by chemical ionization mass spectrometry. *Anal. Chem.*, 78, 6726-6732. doi: 10.1021/ac0604235, 2006.
- 640 Crouse, J.D.; Nielsen, L.B., Jorgensen, S., Kjaergaard, H.G., and Wennberg, P.O.: Autoxidation of Organic Compounds in the Atmosphere, *J. Phys. Chem. Lett.*, 4, 3513–3520, dx.doi.org/10.1021/jz4019207, 2013.
- Di Carlo, P., Brune, W.H., Martinez, M., Harder, H., Leshner, R., Ren, X. R., Thornberry, T., Carroll, M. A., Young, V., Shepson, P. B., Riemer, D., Apel, E., Campbell, C.: Missing OH reactivity in a forest: Evidence for unknown reactive biogenic VOCs, *Science*, 304, 722-725, 2004.
- 645 Diskin, G. S., Podolske, J. R., Sachse, G. W., and Slate, T. A.: Open path airborne tunable diode laser hygrometer. *Diode lasers appl. atmos. sens.*, 4817, 196, International Society for Optics and Photonics. doi: 225 10.1117/12.453736, 2003.
- Fuchs, H., Novelli A., Rolletter M., Hofzumahaus A., Pfannerstill E.Y., Kessel S., Edtbauer A., Williams J., Michoud V., Dusanter S., Locoge N., Zannoni N., Gros V., Truong F., Sarda-Esteve R., Cryer D.R., Brumby C.A., Whalley L.K., Stone D., Seakins P.W., Heard D.E., Schoemaeker C., Blocquet M., Coudert S., Batut S., Fittschen C., Thames A.B., Brune W.H., Ernest C., Harder H., Muller J.B.A., Elste T., Kubistin D., Andres S., Bohn B., Hohaus T., Holland F., Li X., Rohrer F., Kiendler-Scharr A., Tillmann R., Wegener R., Yu Z., Zou Q., Wahner A.: Comparison of OH reactivity measurements in the atmospheric simulation chamber SAPHIR, *Atmos. Meas. Tech.*, 10, 4023–4053, <https://doi.org/10.5194/amt-10-4023-2017>, 2017.
- 655 Goldstein, A. H., Galbally, I. E.: Known and unexplored organic constituents in the Earth's Atmosphere, *Env. Sci. Tech.*, 41(5), 1514–1521, doi:10.1021/es072476p, 2007. Kaiser, J., Skog, K. M., Baumann, K., Bertman, S. B., Brown, S. B., Brune, W. H., Crouse, J. D., de Gouw, J. A., Edgerton, E. S., Feiner, P. A., Goldstein, A. H., Koss, A., Misztal, P. K., Nguyen, T. B., Olson, K. F., St. Clair, J. M., Teng, A. P., Toma, S., Wennberg, P. O., Wild, R. J., Zhang, L. and Keutsch, F. N.: Speciation of OH reactivity above the canopy of an isoprene-dominated forest, *Atmos. Chem. Phys.*, 16(14), 9349–9359, doi:10.5194/acp-16-9349-2016, 2016.
- 660 Jenkin, M. E., Saunders, S. M., Wagner, V., and Pilling, M. J.: Protocol for the development of the Master Chemical Mechanism, MCM v3 (Part B): tropospheric degradation of aromatic volatile organic compounds, *Atmos. Chem. Phys.*, 3, 181-193, <https://doi.org/10.5194/acp-3-181-2003>, 2003.

Formatted: Font:10 pt

Formatted: Default Paragraph Font, Font:(Default) Times New Roman, 10 pt

Formatted: Font:10 pt

Formatted: Indent: Left: 0", Hanging: 0.5", Adjust space between Latin and Asian text, Adjust space between Asian text and numbers

Formatted: Font:(Default) Times New Roman, 10 pt

Formatted: Font:(Default) Times New Roman, 10 pt

Formatted: Font:Italic

Formatted: Font:(Default) Times New Roman, 10 pt

Formatted: Font:(Default) Times New Roman, 10 pt, Not Bold

Formatted: Font:(Default) Times New Roman, 10 pt

Field Code Changed

Formatted: Hyperlink, Font:(Default) Times New Roman, 10 pt

Formatted: Font:(Default) Times New Roman, 10 pt

Formatted: Font:(Default) +Theme Body (Times New Roman), 10 pt, Font color: R,G,B (34,34,34), Pattern: Clear (White)

Deleted: -

Formatted: Font:10 pt

Formatted: Font:10 pt

Formatted: Bibliography, Indent: Left: 0", Hanging: 0.5"

665 Karion, A., Sweeney, C., Wolter, S., Newberger, T., Chen, H., Andrews, A., Kofler, J., Neff, D., and Tans, P.: Long-term
greenhouse gas measurements from aircraft, *Atmos. Meas. Tech.*, *6*, 511–526, <https://doi.org/10.5194/amt-6-511-2013>, 2013.

Burkholder, J.B., Sander, S.P., Abbatt, J., Barker, J.R., Huie, R.E., Kolb, C.E., Kurylo, M.J., Orkin, V.L., Wilmouth, D.,
M., and Wine, P.H.: Chemical Kinetics and Photochemical Data for Use in Atmospheric Studies, Evaluation No.
18, JPL Publication 15-10, Jet Propulsion Laboratory, Pasadena, <http://jpldataeval.jpl.nasa.gov>, 2015.

670 Kaiser, J., Skog, K.M., Baumann, K., Bertman, S.B., Brown, S.B., Brune, W.H., Crounse, J.D., De Gouw, J.A.,
Edgerton, E.S., Feiner, P.A., Goldstein, A.H., Koss, A., Misztal, P.K., Nguyen, T.B., Olson, K.F., St. Clair, J.
M., Teng, A.P., Toma, S., Wennberg, P.O., Wild, R.J., Zhang, L., and Keutsch, F.N.: Speciation of OH reactivity
above the canopy of an isoprene dominated forest, *Atmos. Chem. Phys.*, doi:10.5194/acp-16-9349-2016, 2016.
doi:10.1023/A:1010614113786, 2001.

675 Kovacs, T.A. and Brune, W.H.: Total OH loss rate measurement, *J. Atmos. Chem.*, *39*(2), 105–122,
doi:10.1023/A:1010614113786, 2001.

Kovacs, T.A., Brune, W.H., Harder, H., Martinez, M., Simpas, J.B., Frost, G.J., Williams, E., Jobson, T., Stroud, C.,
Young, V., Fried, A., Wert, B.: Direct measurements of urban OH reactivity during Nashville SOS in summer 1999,
J. Environ. Monitoring, *5* (1), 68–74, 2003.

680 Lana A., Bell T.G., Simó R., Vallina S.M., Ballabrera-Poy J., Kettle A.J., Dachs J., Bopp L., Saltzman E.S., Stefels
J., Johnson J.E., Liss P.S.: An updated climatology of surface dimethylsulfide concentrations and ecampaign fluxes
in the global ocean, *Global Biogeochemical Cycles*, *25*, GB1004, <https://doi.org/10.1029/2010GB003850>, 2011.

Lambe, A.T., Ahern, A.T., Williams, L.R., Slowik, J.G., Wong, J.P.S., Abbatt, J.P.D., Brune, W.H., Ng, N.L., Wright, J.
P., Croasdale, D.R., Worsnop, D.R., Davidovits, P., Onasch, T.B.: Characterization of aerosol photooxidation
685 flow reactors: heterogeneous oxidation, secondary organic aerosol formation and cloud condensation nuclei activity
measurements, *Atmospheric Measurement Techniques*, *4*, 445–461, 10.5194/amt-4-445-2011, 2011.

Maasackers, J.D., Jacob, D.J., Sulprizio, M.P., ScarPELLI, T.R., Nesser, H., Sheng, J.-X., Zhang, Y., Hersher, M., Bloom,
A.A., Bowman, K.W., Worden, J.R., Janssens-Maenhout, G., and Parker, R.J.: Global distribution of methane
emissions, ecampaign trends, and OH concentrations and trends inferred from an inversion of GOSAT satellite data
for 2010–2015, *Atmos. Chem. Phys.*, *19*, 7859–7881, <https://doi.org/10.5194/acp-19-7859-2019>, 2019.

690 Mao J., Ren, X., Brune, W.H., Olson, J.R., Crawford, J.H., Fried, A., Huey, L.G., Cohen, R.C., Heikes, B., Singh, H.B.,
Blake, D.R., Sachse, G.W., Diskin, G.S., Hall, S.R., and Shetter, R.E.: Airborne measurement of OH reactivity
during INTEX-B, *Atmospheric Chemistry and Physics*, *9*, 163–173, 2009.

Millet, D.B., Guenther, A., Siegel, D.A., Nelson, N.B., Singh, H.B., de Gouw, J.A., et al.: Global atmospheric budget of
695 acetaldehyde: 3-D model analysis and constraints from in-situ and satellite observations, *Atmospheric Chemistry
and Physics*, *10*(7), 3405–3425. <https://doi.org/10.5194/acp-10-3405-2010>, 2010.

Naik, V., Voulgarakis, A., Fiore, A.M., Horowitz, L.W., Lamarque, J.-F., Lin, M., Prather, M.J., Young, P.J., Bergmann,
D., Cameron-Smith, P.J., Cionni, I., Collins, W.J., Dalsøren, S.B., Doherty, R., Eyring, V., Faluvegi, G., Folberth,
G.A., Josse, B., Lee, Y.H., MacKenzie, I.A., Nagashima, T., van Noije, T.P.C., Plummer, D.A., Righi, M.,
Rumbold, S.T., Skeie, R., Shindell, D.T., Stevenson, D.S., Strode, S., Sudo, K., Szopa, S., and Zeng, G.:
700 Preindustrial to present-day changes in tropospheric hydroxyl radical and methane lifetime from the Atmospheric
Chemistry and Climate Model Intercomparison Project (ACCMIP), *Atmos. Chem. Phys.*, *13*, 5277–5298,
<https://doi.org/10.5194/acp-13-5277-2013>, 2013.

NASA Earth Observations: <https://neo.sci.gsfc.nasa.gov/>, last access: 5 August 2019.

705 Nicely, J.M., Anderson, D.C., Canty, T.P., Salawitch, R.J., Wolfe, G.M., et al.: An observationally constrained evaluation
of the oxidative capacity in the tropical western Pacific troposphere, *J. Geophys. Res. Atmos.*, *121*, 7461–7488,
doi:10.1002/2016JD025067, 2016.

Neuman, J.A., Trainer, M., Brown, S.S., Min, K.-E., Nowak, J.B., Parrish, D.D., and Veres, P.R.: HONO emission and
production determined from airborne measurements over the Southeast U.S., *J. Geophys. Res. Atmos.*, *121*, 9237–
9250, doi: 10.1002/2016JD025197, 2016.

710 Nölscher, A.C., Williams, J., Sinha, V., Custer, T., Song, W., Johnson, A.M., Axinte, R., Bozem, H., Fischer, H., Povesle,
N., Phillips, G., Crowley, J.N., Rantala, P., Rinne, J., Kulmala, M., Gonzales, D., Valverde-Canossa, J., Vogel, A.,
Hoffmann, T., Ouwensloot, H.G., Vilà-Guerau de Arellano, J. and Lelieveld, J.: Summertime total OH reactivity

Formatted: Font:Times New Roman, 10 pt
Formatted: Font color: Text 1, Pattern: Clear (White)
Formatted: Font:10 pt
Formatted: Font:(Default) +Theme Body (Times New Roman), 10 pt, Font color: Text 1, Pattern: Clear (White)
Deleted: .
Formatted: Font:(Default) +Theme Headings (Times New Roman), 10 pt
Formatted: Default Paragraph Font, Font:(Default) +Theme Headings (Times New Roman), 10 pt
Formatted: Font:(Default) +Theme Headings (Times New Roman), 10 pt
Formatted: Default Paragraph Font, Font:(Default) +Theme Headings (Times New Roman), 10 pt
Formatted: Font:(Default) +Theme Headings (Times New Roman), 10 pt
Formatted: Default Paragraph Font, Font:(Default) +Theme Headings (Times New Roman), 10 pt
Formatted: Font:(Default) +Theme Headings (Times New Roman), 10 pt
Formatted: Default Paragraph Font, Font:(Default) +Theme Headings (Times New Roman), 10 pt
Formatted: Font:(Default) +Theme Headings (Times New Roman), 10 pt
Formatted: Default Paragraph Font, Font:(Default) +Theme Headings (Times New Roman), 10 pt
Formatted: Font:(Default) +Theme Headings (Times New Roman), 10 pt
Formatted: Default Paragraph Font, Font:(Default) +Theme Headings (Times New Roman), 10 pt
Formatted: Font:(Default) +Theme Headings (Times New Roman), 10 pt
Formatted: Default Paragraph Font, Font:(Default) +Theme Headings (Times New Roman), 10 pt
Formatted: Font:(Default) +Theme Headings (Times New Roman), 10 pt
Formatted: Default Paragraph Font, Font:(Default) +Theme Headings (Times New Roman), 10 pt
Formatted: Font:(Default) +Theme Headings (Times New Roman), 10 pt
Formatted: Font:(Default) +Theme Headings (Times New Roman), 10 pt
Formatted: Font:(Default) +Theme Headings (Times New Roman), 10 pt
Formatted: Font:(Default) +Theme Headings (Times New Roman), 10 pt
Formatted: Font:(Default) +Theme Headings (Times New Roman), 10 pt
Formatted: Font:(Default) +Theme Headings (Times New Roman), 10 pt
Formatted: Font:(Default) +Theme Headings (Times New Roman), 10 pt
Formatted: Font:(Default) +Theme Headings (Times New Roman), 10 pt
Formatted: Font:10 pt
Formatted: Default Paragraph Font, Font:10 pt
Formatted: Font:10 pt

715 measurements from boreal forest during HUMPPA-COPEC 2010, *Atmos. Chem. Phys.*, 12(17), 8257–8270, doi:10.5194/acp-12-8257-2012, 2012.

Nölscher, A. C., Yañez-Serrano, A. M., Wolff, S., de Araujo, A. C., Lavrič, J. V., Kesselmeier, J. and Williams, J.: Unexpected seasonality in quantity and composition of Amazon rainforest air reactivity, *Nature Communications*, 7(1), doi:10.1038/ncomms10383, 2016.

720 Pfannerstill, E. Y., Wang, N., Edtbauer, A., Bourtoukoudis, E., Crowley, J. N., Dienhart, D., Eger, P. G., Ernle, L., Fischer, H., Hottmann, B., Paris, J.-D., Stöner, C., Tadic, I., Walter, D., Lelieveld, J., and Williams, J.: Shipborne measurements of total OH reactivity around the Arabian Peninsula and its role in ozone chemistry, *Atmos. Chem. Phys.*, 19, 11501–11523, <https://doi.org/10.5194/acp-19-11501-2019>, 2019.

725 Pozzer, A., Pollmann, J., Taraborrelli, D., Jockel, P., Helmig, D., Tans, P., Hueber, J., Lelieveld, J.: Observed and simulated global distribution and budget of atmospheric C2–C5 alkanes. *Atmos. Chem. Phys.*, 10, 4403–4422, 2010.

Prather, M. J., Holmes, C. D., and Hsu, J.: Reactive greenhouse gas scenarios: Systematic exploration of uncertainties and the role of atmospheric chemistry, *Geophys. Res. Lett.*, 39, L09803, doi:10.1029/2012GL051440, 2012.

Read, K. A., Carpenter, L. J., Arnold, S. R., Beal, R., Nightingale, P. D., Hopkins, J. R., Lewis, A. C., Lee, J. D., Mendes, L., Pickering, S. J.: Multiannual Observations of Acetone, Methanol, and Acetaldehyde in Remote Tropical Atlantic Air: Implications for Atmospheric OVOC Budgets and Oxidative Capacity, *Environ. Sci. Tech.*, 46, 11028–11039, dx.doi.org/10.1021/es302082p, 2012.

730 Ryerson, T. B., Williams, E. J., and Fehsenfeld, F. C.: An efficient photolysis system for fast response NO₂ measurements. *J. Geophys. Res. Atmos.*, 105, 26447–26461. doi: 10.1029/2000JD900389, 2000.

735 Santoni, G. W., Daube, B. C., Kort, E. A., Jimenez, R., Park, S., Pittman, J. V., Wofsy, S. C.: Evaluation of the airborne quantum cascade laser spectrometer (QCLS) measurements of the carbon and greenhouse gas suite - CO₂, CH₄, N₂O, and CO - during the CalNex and HIPPO Campaigns, *Atmos. Meas. Tech.*, 7, 1509–1526. doi: 10.5194/amt-7-1509-2014, 2014.

740 Saunders, S. M., Jenkin, M. E., Derwent, R. G., and Pilling, M. J.: Protocol for the development of the Master Chemical Mechanism, MCM v3 (Part A): tropospheric degradation of non-aromatic volatile organic compounds, *Atmos. Chem. Phys.*, 3, 161–180, <https://doi.org/10.5194/acp-3-161-2003>, 2003.

Shetter, R. E. and Mueller, M.: Photolysis frequency measurements using actinic flux spectroradiometry during the PEM-Tropics mission: Instrumentation description and some results, *J. Geophys. Res. Atmos.*, 104, 5647–5661. doi: 10.1029/98JD01381, 1999.

745 Singh H.B., Salas L.J., Chatfield R.B., Czech, E., Fried A., Walega J., Evans M.J., Field B.D., Jacob D.J., Blake D., Heikes B., Talbot R., Sachse G., Crawford J. H., Avery M.A., Sandholm S., Fuelberg H.: Analysis of the atmospheric distribution, sources, and sinks of oxygenated volatile organic chemicals based on measurements over the Pacific during TRACE-P, *Journal of Geophysical Research*: 109, D15S07, <https://doi.org/10.1029/2003JD003883>, 2004.

Tokarek, T. W., Brownsey, D. K., Jordan, N., Garner, N. M., Ye, C. Z., Osthoff, H. D.: Emissions of C₉ – C₁₆ hydrocarbons from kelp species on Vancouver Island: *Alaria marginata* (winged kelp) and *Nereocystis luetkeana* (bull kelp) as an atmospheric source of limonene, *Atmos. Environ. X*, 2, Article 100007, 2019.

750 Travis, K. R., Heald, C. L., Allen, H. M., Apel, E. C., Arnold, S. R., Blake, D. R., Brune, W. H., Chen, X., Commane, R., Crouse, J. D., Daube, B. C., Diskin, G. S., Elkins, J. W., Evans, M. J., Hall, S. R., Hints, E. J., Hornbrook, R. S., Kasibhatla, P. S., Kim, M. J., Luo, G., McKain, K., Millet, D. B., Moore, F. L., Peischl, J., Ryerson, T. B., Sherwen, T., Thames, A. B., Ullmann, K., Wang, X., Wennberg, P. O., Wolfe, G. M., and Yu, F.: Constraining remote oxidation capacity with ATom observations, *Atmos. Chem. Phys. Discuss.*, <https://doi.org/10.5194/acp-2019-931>, in review, 2020.

755 Wang, S., Hornbrook, R. S., Hills, A., Emmons, L. K., Tilmes, S., Lamarque, J.-F., et al.: Atmospheric acetaldehyde: Importance of air-sea exchange and a missing source in the remote troposphere. *Geophysical Research Letters*, 46, 5601–5613. <https://doi.org/10.1029/2019GL082034>, 2019.

760 Wofsy, S.C., S. Afshar, H.M. Allen, E. Apel, E.C. Asher, B. Barletta, J. Bent, H. Bian, B.C. Biggs, D.R. Blake, N. Blake, I. Bourgeois, C.A. Brock, W.H. Brune, J.W. Budney, T.P. Bui, A. Butler, P. Campuzano-Jost, C.S. Chang, M. Chin, R. Commane, G. Correa, J.D. Crouse, P. D. Cullis, B.C. Daube, D.A. Day, J.M. Dean-Day, J.E. Dibb, J.P. DiGangi, G.S. Diskin, M. Dollner, J.W. Elkins, F. Erdesz, A.M. Fiore, C.M. Flynn, K. Froyd, D.W. Gesler, S.R. Hall, T.F. Hanisco, R.A. Hannun, A.J. Hills, E.J. Hints, A. Hoffman, R.S. Hornbrook, L.G. Huey, S. Hughes, J.L.

Formatted: Font:10 pt

Deleted:

Deleted: Discuss., <https://doi.org/10.5194/acp-2019-416>, in review

Formatted: Font:10 pt

Formatted: Font:10 pt

Deleted: .

Formatted: Font:10 pt

Formatted: Indent: Left: 0", First line: 0"

Formatted: Default Paragraph Font, Font:(Default) Times New Roman, 10 pt, Font color: Auto, Pattern: Clear

Formatted: Font:10 pt

Formatted: Bibliography, Indent: Left: 0", Hanging: 0.5"

Formatted: Font:(Default) +Theme Headings (Times New Roman), 10 pt

Formatted: Font:(Default) +Theme Headings (Times New Roman)

Deleted: .

Formatted: Font:(Default) Times New Roman

Formatted: Font:10 pt

770 [Jimenez, B.J. Johnson, J.M. Katich, R.F. Keeling, M.J. Kim, A. Kupc, L.R. Lait, J.-F. Lamarque, J. Liu, K. McKain, R.J. Mclaughlin, S. Meinardi, D.O. Miller, S.A. Montzka, F.L. Moore, E.J. Morgan, D.M. Murphy, L.T. Murray, B.A. Nault, J.A. Neuman, P.A. Newman, J.M. Nicely, X. Pan, W. Paplawsky, J. Peischl, M.J. Prather, D.J. Price, E. Ray, J.M. Reeves, M. Richardson, A.W. Rollins, K.H. Rosenlof, T.B. Ryerson, E. Scheuer, G.P. Schill, J.C. Schroder, J.P. Schwarz, J.M. St.Clair, S.D. Steenrod, B.B. Stephens, S.A. Strode, C. Sweeney, D. Tanner, A.P. Teng, A.B. Thames, C.R. Thompson, K. Ullmann, P.R. Veres, N. Vieznor, N.L. Wagner, A. Watt, R. Weber, B. Weinzierl, P. Wennberg, C.J. Williamson, J.C. Wilson, G.M. Wolfe, C.T. Woods, and L.H. Zeng; ATom: Merged Atmospheric Chemistry, Trace Gases, and Aerosols, ORNL DAAC, Oak Ridge, Tennessee, USA. <https://doi.org/10.3334/ORNLDAAC/1581>, 2018.](#)

775

780 Wolfe, G.M, Marvin, M.R., Roberts, S.J., Travis, K.R., and Liao, J.: The Framework for 0-D Atmospheric Modeling (F0AM) v3.1, Geosci. Model Dev., 9, 3309-3319, doi: 10.5194/gmd-9-3309-2016, 2016.

785 Yang, Y, Shao, M., Wang, X., Noelscher, A.C., Kessel, S., Guenther, A., Williams, J.: Towards a quantitative understanding of total OH reactivity: A review, Atmos. Environ., 143, 147-161, 2016.

Zannoni, N., Gros, V., Lanza, M., Sarda, R., Bonsang, B., Kalogridis, C., Preunkert, S., Legrand, M., Jambert, C., Boissard, C., Lathiere, J.: OH reactivity and concentrations of biogenic volatile organic compounds in a Mediterranean forest of downy oak trees, Atmos. Chem. Phys., 16(3), 1619–1636, doi:10.5194/acp-16-1619-2016, 2016.

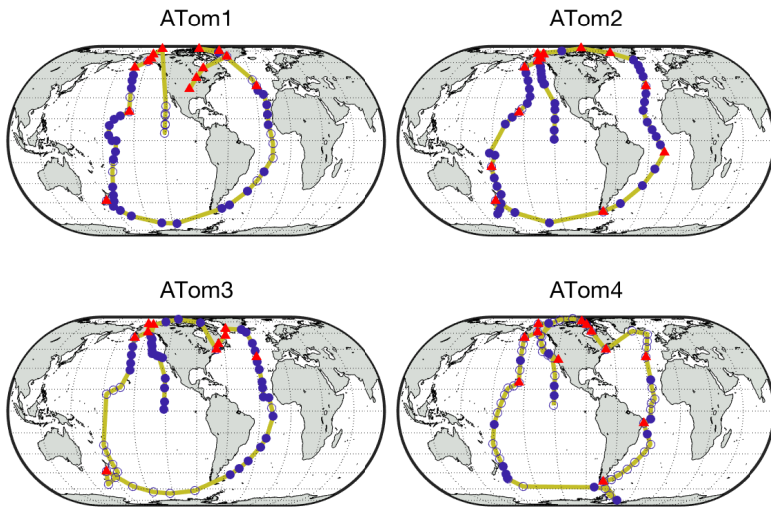
Formatted: Font:10 pt

Formatted: Font:10 pt

Formatted: Hyperlink, Font:10 pt, Pattern: Clear

Formatted: Font:10 pt

Field Code Changed



790 Figure 1: Global ATom tracks (yellow lines) with indicators for the periods during which the DC-8 dipped into the boundary layer. Filled blue circles indicate points used for analysis; filled red triangles indicate dips when over land; unfilled blue circles indicate dips not used for analysis due to instrument calibrations or downtime.

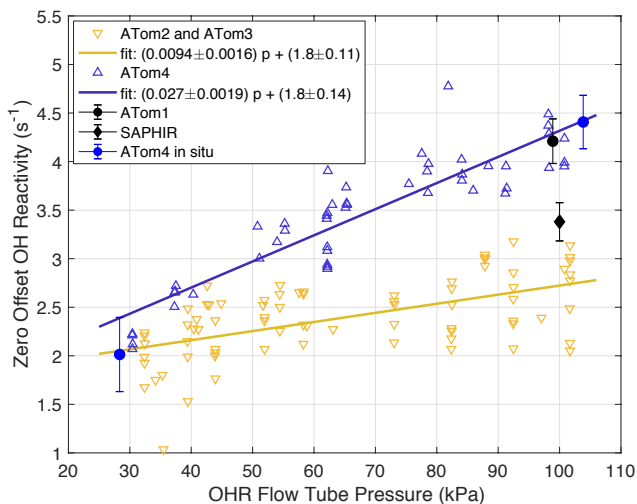
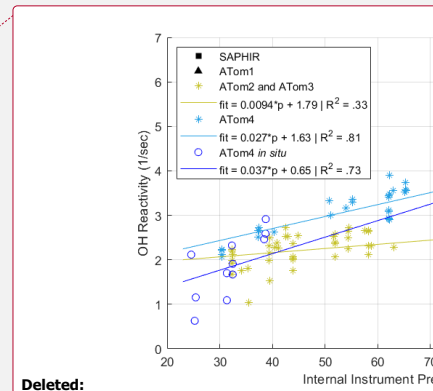


Figure 2. Laboratory and in situ calibrations of OHR offset over 1-minute sums. The offset was calibrated only at ~100 kPa around ATom1 in 2015 and 2016 (black triangle). The offset was measured with a slightly different instrument configuration during the OH reactivity intercomparison study in 2015 (Fuchs et al., 2017). Offset calibrations performed in 2017 between ATom2 and ATom3 (yellow stars with linear fit (yellow line), in 2018 at the end of ATom4 (red circles) and linear fit (red line), and in flight are shown. Error bars are ± 1 standard deviation of the mean. The ATom4 fit was used for ATom1 because the high-pressure laboratory calibrations were essentially the same.

800



Deleted:

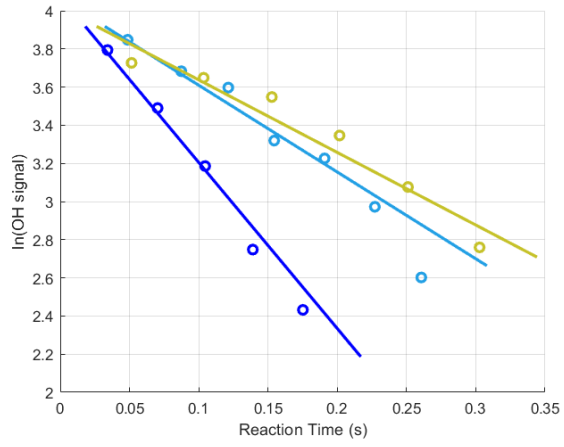
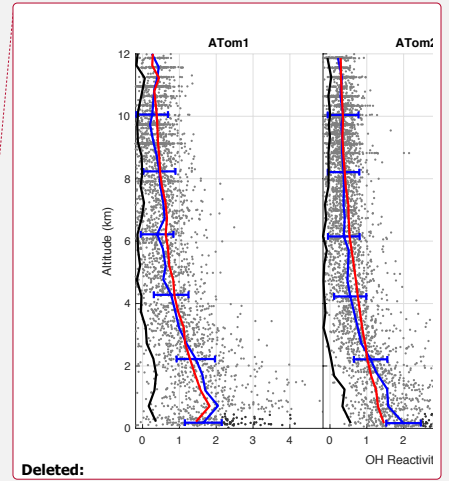
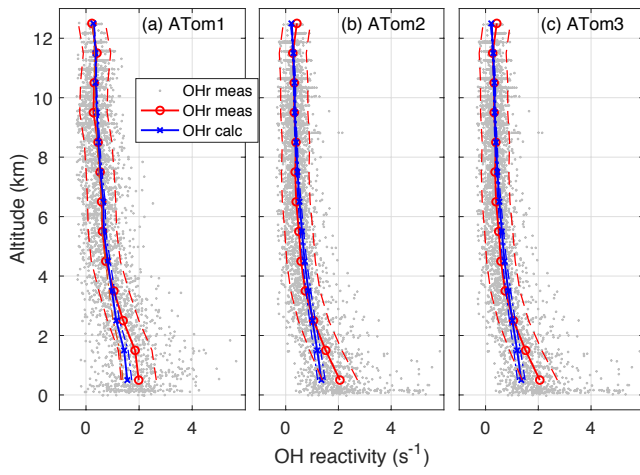


Figure 3: Three in-flight decays for 1-minute sums of the OH signals. Decays were measured in the marine boundary layer and the individual 5 Hz data were binned by reaction times for clarity. When k_{offset} is subtracted from the decays, their values become ~ 5 s^{-1} (blue), ~ 3 s^{-1} (teal), and ~ 2 (yellow) s^{-1} .

810

Deleted: background



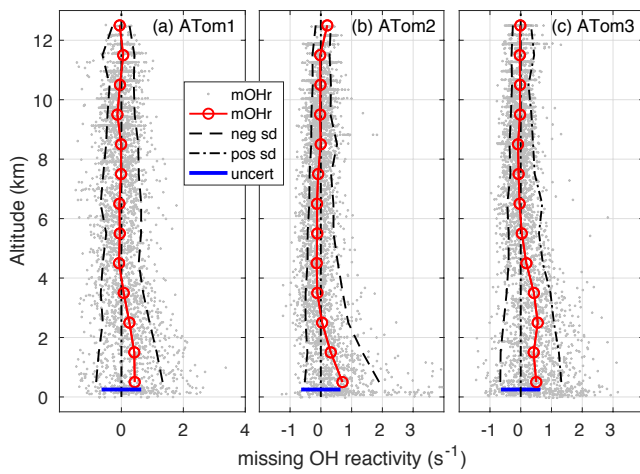
815 **Figure 4. OH reactivity versus altitude for ATom1 (August), ATom2 (February), and ATom3 (October). 1-minute measured OH reactivity (grey dots), median measured OH reactivity (Ohr meas) in 1-km altitude bins (red circle and line), and median calculated OH reactivity (Ohr calc) in 1-km altitude bins (blue squares and line), and absolute OHR uncertainty (95% confidence level) for measured and calculated OH reactivity (dashed lines) are shown as a function of altitude.**

Deleted: each ATom campaign

Deleted: The grey points represent each 1-minute measured OHR value with the instrument offset and internal contamination removed.

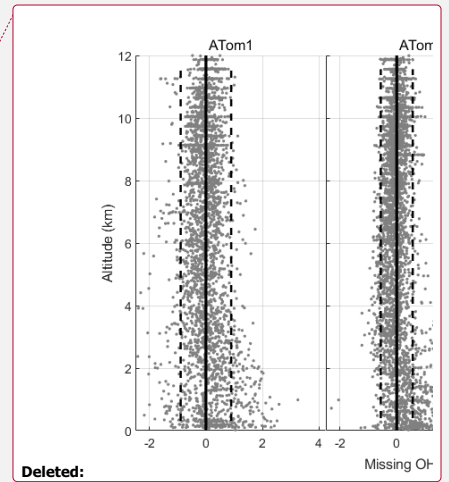
Deleted:

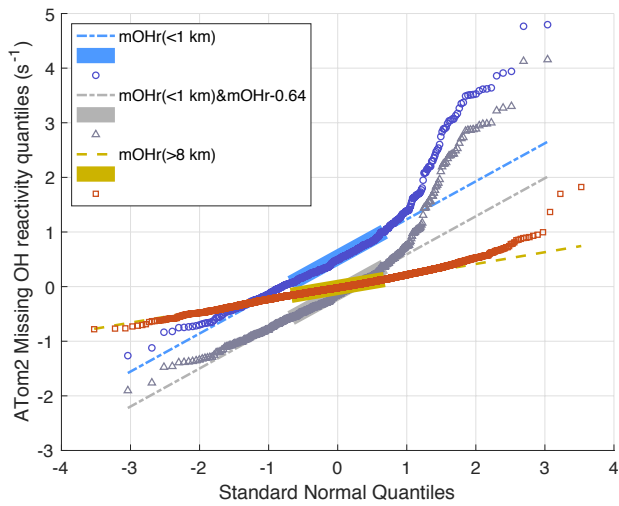
Deleted: The median OH reactivity of 500m altitude bins is shown for measured OH reactivity (blue line, with 1 σ error bars), for model-calculated OH reactivity (red line), and for missing OH reactivity (black line). Darker grey points indicate OH reactivity values greater than the 1 σ uncertainty in the MBL.



835 **Figure 5: Missing OH reactivity (mOHr) against altitude for ATom1 (August), ATom2 (February), and ATom3 (October). Grey dots are the OH reactivity calculated by subtracting calculated OH reactivity from measured OH reactivity. Median missing OH reactivity below 1 km altitude (red circles and lines) is comparable to the absolute uncertainty in the missing OH reactivity (blue bar, 95% confidence). The standard deviation of the negative missing OH reactivity data for each 1-km of altitude (left of the zero line) and of the positive missing OH reactivity data (right of the zero line) are shown at the 95% confidence level and indicate the skewness in the missing OH reactivity data distribution below 2-4 km altitude.**

840

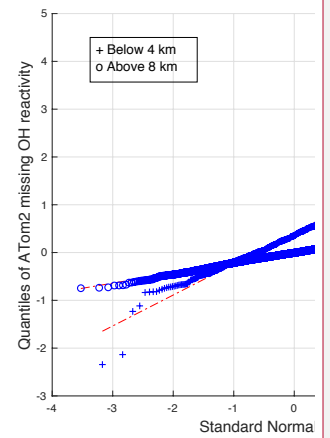




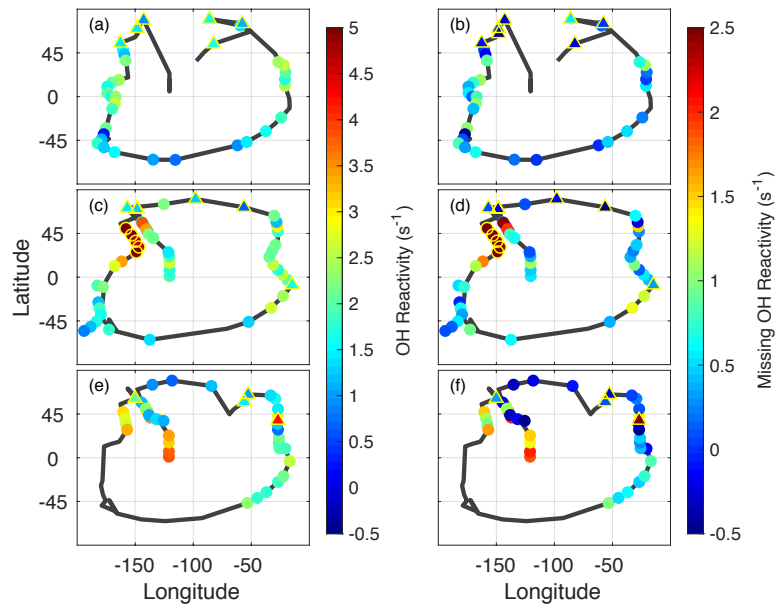
845 **Figure 6:** ATom2 quantile-quantile plot for 1-minute missing OH reactivity values above 8 km (red squares) and below 1 km (blue circles) versus a normal distribution with a mean of 0 and a standard deviation of 1. The Q-Q plot for data taken below 1 km but with the median value shifted by 0.64 s^{-1} (gray triangles) show the effect of an incorrect absolute missing OH reactivity median. The values lie along the dashed lines if the missing OH reactivity values are normally distributed. This Q-Q plot is for ATom2; the Q-Q plots for ATom1 and ATom3 show less dramatic but similar behavior to that of ATom2.

850

Formatted: Superscript

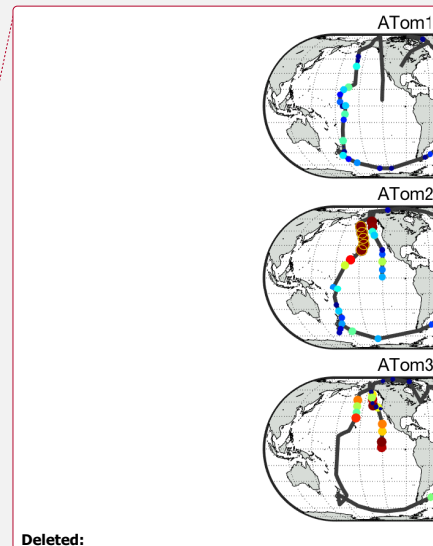


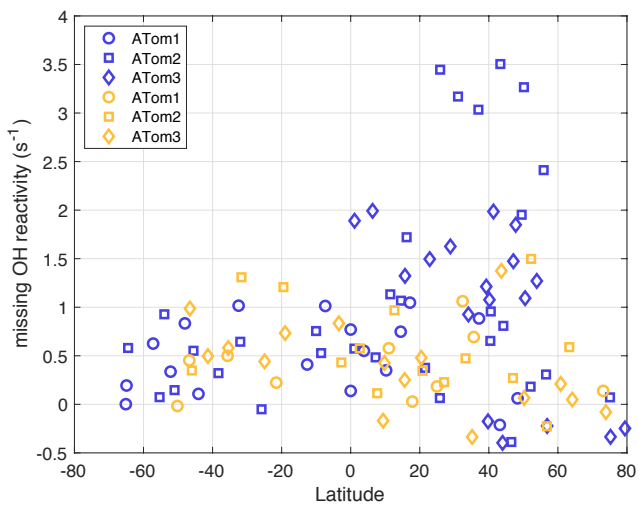
Deleted:



855 **Figure 7. Global measured OH reactivity (a, c, and e) and missing OH reactivity (b, d, and f) for ATom1 (August), ATom2**
(February), and ATom3 (October) at the per-dip time resolution. The black lines trace the flight path during each deployment,
identical to the yellow tracks in Figure 1. Color indicates the measured OH reactivity (-0.5 to 5 s⁻¹ scale) and the missing OH
reactivity (-0.5 to 2.5 s⁻¹ scale), while the yellow open circles indicate values in ATom2 above 2 s⁻¹ that were not included in the
correlation analysis. Triangles outlined by yellow are overland values for both measured OH reactivity and missing OH reactivity.

860





Formatted: Centered

865 **Figure 8.** Missing OH reactivity averaged per-dip versus latitude over the Pacific Ocean (blue) and the Atlantic Ocean (gold).

Formatted: Font:9 pt, Bold

Formatted: Font:9 pt, Bold

Formatted: Font:9 pt, Bold

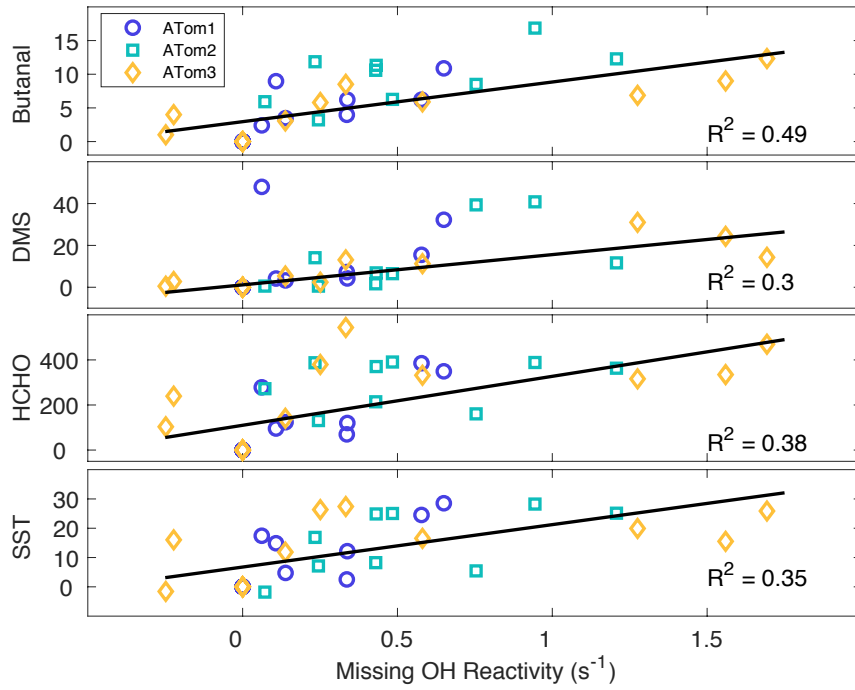


Figure 8. The best correlations with missing OH reactivity for data at the per-flight resolution across all latitudes and hemispheres. The symbols are per-flight data for ATom1 (circles), ATom2 (squares), ATom3 (diamonds). Black lines are least squares fits to the per-flight data.

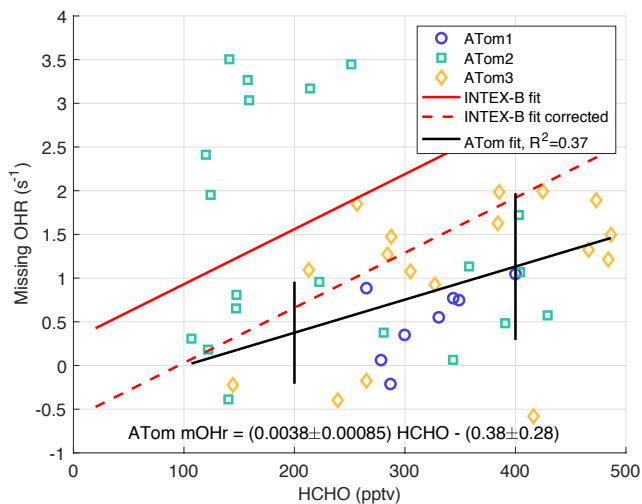
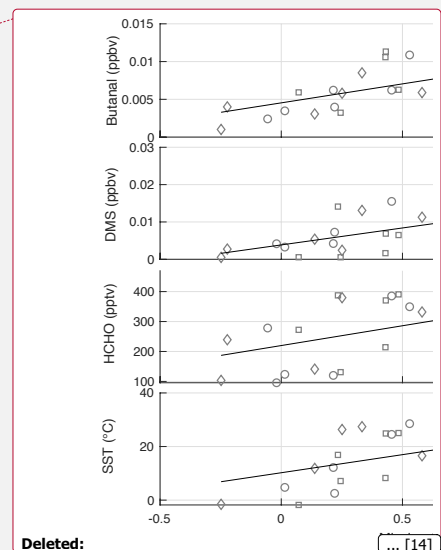
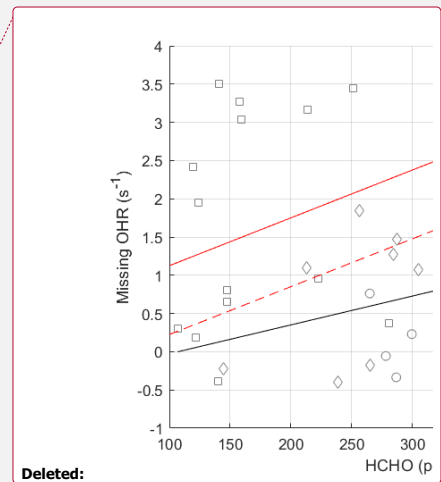


Figure 9. Missing OH reactivity against HCHO for per-dip values in the MBL over the Northern Hemisphere Pacific Ocean. The ATom linear fit (black line) is shown with values for ATom1 (circles), ATom2 (squares), ATom3 (diamonds). The ATom linear fit is compared to the linear fit for missing OH reactivity values of Mao et. al (2009) (red line) and to this linear fit with an offset correction (red dashed line, see text). Uncertainty bars are the absolute uncertainty (95% confidence) of the missing OH reactivity. The statistical uncertainty in the slope and intercept of the linear fit are given in the equation on the figure.



Deleted: ... [14]



Deleted:

Table 1: ATom campaign deployment seasons and start and end dates. Full details on stops can be found online (ATom, 2016).

Deployment	ATom1	ATom2	ATom3	ATom4
NH Season	Summer	Winter	Fall	Spring
Start Date	28 July 2016	26 Jan 2017	28 Sept 2017	24 Apr 2018
End Date	22 August 2016	22 Feb 2017	26 Oct 2017	21 May 2018

- Deleted: Phase
- Formatted Table
- Formatted: Left

890

Table 2. Simultaneous measurements used to constrain the box model and calculate OH reactivity.

Measurement	Instrument	Uncertainty (2σ confidence)	Reference
T	MMS	± 0.5 C	Chan et al., 1998
p		± 0.3 hPa	
H ₂ O	DLH	$\pm 15\%$	Diskin et al., 2003
photolysis frequencies (30 measurements)	CAFS	$\pm (12-25)\%$, species dependent	Shetter and Mueller, 1999
NO, NO ₂	NOyO3	6.6 pptv, 34 pptv	Ryerson et al., 2000
O ₃	NOyO3 [#] UCATS	1.4 ppbv $\pm 1\% + 1.5$ ppbv	Ryerson et al., 2000
CO	QCLS [#] NOAA Picarro UCATS	3.5 ppbv 3.6 ppbv 8.4 ppbv	Santorini et al., 2014 H. Chen et al., 2013
H ₂ O ₂ , CH ₃ OOH, CH ₃ CO ₃ H, HNO ₃ SO ₂	CIT CIMS	$\pm 30\% + 50$ pptv $\pm 30\% + 100$ pptv	Crouse et al., 2006
HCOOH, BrO	NOAA CIMS	$\pm 15\% + 50$ pptv	Neuman et al., 2016
CH ₄	NOAA Picarro [#] UCATS PANTHER	0.7 ppbv 23.6 ppbv 34.6 ppbv	Karion et al., 2013
HCHO	NASA ISAF	$\pm 10\% \pm 10$ pptv	Cazorla et al., 2015
methyl nitrate, ethyl nitrate, isoprene, acetylene, ethylene, ethane, propane, i-butane, n-butane, i- pentane, n-pentane, n- hexane, n-heptane, benzene, toluene, methyl chloride, methylene chloride, chloroform, methyl bromide, methyl chloroform, perchloroethene, 1,2- dichloroethane, DMS	UCI WAS	$\pm 10\%$	Colman et al., 2001
methanol, formaldehyde, acetaldehyde, ethyl benzene, toluene, methacrolein, methyl ethyl ketone, methyl tert-butyl ether, ethanol, acetone, 2- methylpentane, 3- methylpentane, 2,2,4- trimethylpentane, isobutene+1-butene, m- xylene+p-xylene, o-xylene, tricyclene, limonene+D3- carene, propanal, butanal, acrolein	TOGA	$\pm 15-50\%$ (acetaldehyde: $\pm 20\%$)	Apel et al., 2015

Formatted Table

Formatted: Subscript

Deleted: H. Chen et al., 2013

Table 3: Simple X photochemistry added to the photochemical mechanism to test for effects of X on modeled OH and HO₂

Reaction	Reaction rate coefficient (cm ³ s ⁻¹)
case 1: X + OH → XO ₂	1x10 ⁻¹⁰
case 2: X + OH → XO ₂ + OH	
X + O ₃ → XO ₂	1x10 ⁻¹⁶
XO ₂ + NO → HO ₂ + NO ₂ + prod	3x10 ⁻¹² exp (300/T)
XO ₂ + HO ₂ → XOOH	8.6x10 ⁻¹³ exp (700/T)
XOOH + hv → XO + OH	J _{CH₃O₂H} (s ⁻¹)
XOOH + OH → XO ₂	2.9x10 ⁻¹² exp (-160/T)

Formatted Table

Alexander B. Thames¹, William H. Brune¹, David O. Miller¹, Hannah M. Allen⁴, Eric C. Apel², Donald R. Blake¹⁵, T. Paul Bui⁸, Roisin Commane¹⁴, John D. Crouse⁴, Bruce C. Daube¹³, Glenn S. Diskin⁵, Joshua P. DiGangi⁵, James W. Elkins¹⁰, Samuel R. Hall², Thomas F. Hanisco⁶, Reem A. Hannun^{6,7}, Eric Hints^{10,12}, Rebecca S. Hornbrook², Michelle J. Kim³, Kathryn McKain^{10,12}, Fred L. Moore^{10,12}, Julie M. Nicely^{6,7}, Jeffrey Peischl^{10,11}, Thomas B. Ryerson¹¹, Jason M. St. Clair^{6,7}, Colm Sweeney⁹, Alex Teng⁴, Chelsea R. Thompson^{16,11,12}, Kirk Ullmann², Paul O. Wennberg³, and Glenn M. Wolfe^{6,7}

¹Department of Meteorology and Atmospheric Science, The Pennsylvania State University, University Park, PA, USA.

²Atmospheric Chemistry Observations and Modeling Laboratory, National Center for Atmospheric Research, Boulder, CO, USA.

³Division of Geological and Planetary Sciences, California Institute of Technology, Pasadena, CA, USA.

⁴Division of Chemistry and Chemical Engineering, California Institute of Technology, Pasadena, CA, USA.

⁵Chemistry and Dynamics Branch, NASA Langley Research Center, Hampton, VA, USA.

⁶Atmospheric Chemistry and Dynamics Laboratory, NASA Goddard Space Flight Center, Greenbelt, MD, USA.

⁷Joint Center for Earth Systems Technology, University of Maryland, Baltimore County, Catonsville, MD, USA.

⁸Earth System Science Interdisciplinary Center, University of Maryland, College Park, MD, USA

⁹Earth Science Division, NASA Ames Research Center, Moffett Field, CA, USA.

¹⁰Global Monitoring Division, NOAA Earth System Research Laboratory, Boulder, CO, USA.

¹¹Chemical Sciences Division, NOAA Earth System Research Laboratory, Boulder, CO, USA.

¹²Cooperative Institute for Research in Environmental Sciences, University of Colorado, Boulder, CO, USA.

¹³Department of Earth and Planetary Sciences, Harvard University, Cambridge, MA, USA.

¹⁴Department of Earth and Environmental Sciences, Lamont-Doherty Earth Observatory, Columbia University, Palisades, NY, USA.

¹⁵Department of Chemistry, University of California, Irvine, CA, USA.

¹⁶Now with Scientific Aviation, Boulder, CO, USA.

All calibrations are pressure-dependent, with all three background calibrations being the same to within 0.5 s^{-1} at 300 hPa instrument flow tube pressure, which is approximately 10 km altitude.

At all pressures, the background calibration data indicate that the backgrounds are known to $\pm 0.4 \text{ s}^{-1}$ at 1σ confidence. The uncertainty in decay fit is approximately 7.5% at the 1σ confidence level, such that the total uncertainty can be found by Eq. (4).

$$\Delta = \quad (4)$$

For example, for a measured decay of 5 s^{-1} , the resulting uncertainty would be $\pm 0.55 \text{ s}^{-1}$ at 1σ confidence.

If these values were purely normal distributions, as would be expected from a missing OH reactivity created solely by the instrument uncertainty, then they would lie along the red dashed lines. Values higher than the red dashed line indicate that the number of missing OH reactivity

values in that part of the distribution is much greater than would be expected for a normal distribution. The missing OH reactivity values measured below 4 km altitude lie along the red dashed line, which passes through (0.0, 0.0), indicating that the median value is 0 s^{-1} and the values follow the normal distribution. However, while more than 90% of the missing OH reactivity values below 4 km follow the normal distribution, there are many missing OH reactivity values that fall above those predicted by a strictly normal distribution. This deviation from a normal distribution indicates that the missing OH reactivity exceeds the statistical error range.

A Student t-test also determines whether the missing OH reactivity from the lowest 4 km is statistically consistent with the normally distributed points above 4 km. For each campaign, the calculated p-values are below 10^{-5} . As a result, we can reject the null hypothesis that the missing OH reactivity in the lower troposphere comes from the same distribution as those in the upper troposphere. These two tests provide statistical evidence that the observed missing OH reactivity is significant.

Page 36: [5] Formatted	William Brune	1/25/20 11:14:00 AM
Font:(Default) +Theme Headings (Times New Roman), 10 pt		
Page 36: [6] Formatted	William Brune	1/25/20 11:14:00 AM
Default Paragraph Font, Font:(Default) +Theme Headings (Times New Roman), 10 pt		
Page 36: [7] Formatted	William Brune	1/25/20 11:14:00 AM
Font:(Default) +Theme Headings (Times New Roman), 10 pt		
Page 36: [8] Formatted	William Brune	1/25/20 11:14:00 AM
Default Paragraph Font, Font:(Default) +Theme Headings (Times New Roman), 10 pt		
Page 36: [9] Formatted	William Brune	1/25/20 11:14:00 AM
Font:(Default) +Theme Headings (Times New Roman), 10 pt		
Page 36: [10] Formatted	William Brune	1/25/20 11:14:00 AM
Default Paragraph Font, Font:(Default) +Theme Headings (Times New Roman), 10 pt		
Page 36: [11] Formatted	William Brune	1/25/20 11:14:00 AM
Font:(Default) +Theme Headings (Times New Roman), 10 pt		
Page 36: [12] Formatted	William Brune	1/25/20 11:14:00 AM
Default Paragraph Font, Font:(Default) +Theme Headings (Times New Roman), 10 pt		
Page 36: [13] Formatted	William Brune	1/25/20 11:14:00 AM
Font:(Default) +Theme Headings (Times New Roman), 10 pt		
Page 48: [14] Deleted	William Brune	1/22/20 11:23:00 AM

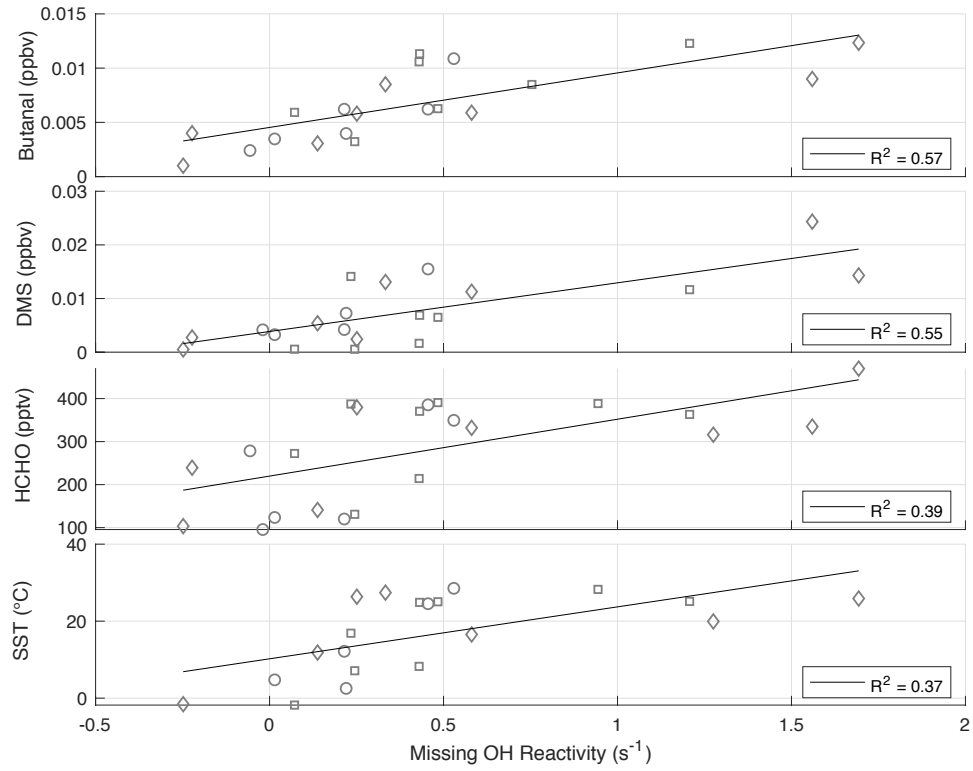


Figure 8. The best correlations with missing OH reactivity at the per-flight time resolution across all latitudes and hemispheres. The symbols are values for ATom1 (circles), ATom2 (squares), ATom3 (diamonds).